PERIOCULAR RECOGNITION IN CROSS-SPECTRAL SCENARIO

M.Tech. Thesis

By

SUSHREE SANGEETA BEHERA

DISCIPLINE OF ELECTRICAL ENGINEERING

INDIAN INSTITUTE OF TECHNOLOGY INDORE

JUNE 2017

PERIOCULAR RECOGNITION IN CROSS-SPECTRAL SCENARIO

A THESIS

Submitted in partial fulfillment of the requirements for the award of the degree

of

Master of Technology

by

SUSHREE SANGEETA BEHERA

DISCIPLINE OF ELECTRICAL ENGINEERING

INDIAN INSTITUTE OF TECHNOLOGY INDORE

JUNE 2017

INDIAN INSTITUTE OF TECHNOLOGY INDORE

CANDIDATE'S DECLARATION

I hereby certify that the work which is being presented in the thesis entitled **PERIOCULAR RECOGNITION IN CROSS-SPECTRAL SCENARIO** in the partial fulfillment of the requirements for the award of the degree of **MASTER OF TECHNOLOGY** and submitted in the **DISCIPLINE OF ELECTRICAL ENGINEERING, Indian Institute of Technology Indore**, is an authentic record of my own work carried out during the time period from July 2015 to June 2017 under the supervision of Dr. Vivek Kanhangad, Associate Professor, IIT Indore.

The matter presented in this thesis has not been submitted by me for the award of any other degree of this or any other institute.

Signature of the student with date
(SUSHREE SANGEETA BEHERA)

This is to certify that the above statement made by the candidate is correct to the best of my knowledge.

Signature of the Supervisor of
M.Tech. thesis (with date)
(Dr. VIVEK KANHANGAD)

SUSHREE SANGEETA BEHERA has successfully given her M.Tech. Oral Examination held on **27th June 2017**.

Signature of Supervisor of M.Tech. thesis
Date:

Convener, DPGC
Date:

Signature of PSPC Member #1
Date:

Signature of PSPC Member #2
Date:

Dedicated

to

My Parents

Acknowledgments

I express my deep sense of gratitude to Almighty for guiding me and giving patience throughout this duration. This venture has received the hearty support of my guide Dr. Vivek Kanhangad. His constant encouragement, motivation and enthusiasm helped me to move forward with investigation in depth.

I am extremely happy to express my gratitude towards my PG student's progress committee members Dr. R. B. Pachori and Dr. Surya Prakash for their guidance and support. I am thankful to Dr. Trapti Jain, HOD, Dept. of Electrical Engineering for her support and cooperation. I am thankful to all the faculty members of the department of Electrical Engineering for their guidance and support.

I express my gratitude to members of pattern recognition and image analysis group to provide me such a platform to learn various softwares related to image processing. I am very thankful to T. Sunil, Vijay, Mahesh, Ankita and Shishir who contributed significantly to this thesis work. Their valuable suggestions helped me to gain extra knowledge in MATLAB and achieve the results faster.

I cannot forget the support and encouragement received from my parents, brother, friends and family, without whom this journey would not have been possible.

Sushree Sangeeta Behera

Abstract

Periocular recognition has been an active area of research in the past few years due to its potential use in practical security applications. In spite of the advancements made in this area, the cross-spectral matching of visible (VIS) and near-infrared (NIR) periocular images remains a challenge. In this work, we propose a method based on illumination normalization of VIS and NIR periocular images. Specifically, the approach involves normalizing the images using the difference of Gaussian (DoG) filtering, followed by the computation of various texture based and shape based descriptors.These features include local binary patterns (LBP), histogram of oriented gradients (HOG), Gabor filter based features and local phase quantisation (LPQ) based features. Finally, the feature vectors corresponding to the query and the enrolled image are compared using the cosine similarity metric (COS) to generate a matching score. Both verification and identification experiments are performed on three publicly available benchmark databases of cross-spectral periocular images, which include IIIT Delhi multi-spectral periocular (IMP) database, PolyU cross-spectral iris database and cross-eyed periocular database. We have also investigated the performance of other existing illumination normalization methods on these databases. Our approach yields significant improvement in performance (verification accuracy) over the existing approach. We have also developed an in-house database of cross-spectral periocular images. This database includes VIS and NIR images of the left and right periocular images of 201 subjects. The performance of the proposed approach is also evaluated on this database for both verification and identification scenarios.

Contents

List of Figures

List of Tables

List of Abbreviations

BSIF	Binarized Statistical Image Features
CLAHE	Contrast Limited Adaptive Histogram Equalization
CMC	Cumulative Match Curve
CRBM	Convolutional Restricted Boltzman Machine
COS	Cosine metric
DLDA	Direct Linear Discriminant Analysis
DoG	Difference of Gaussian
DVS	Digital Video Server
EER	Equal Error Rate
FAR	False Acceptance Rate
GAR	Genuine Acceptance Rate
HOG	Histogram of Oriented Gradients
ICA	Independent Component Analysis
IMP	IIIT Delhi Multi-spectral Periocular
IR	Infra-Red
LBP	Local Binary Pattern
LDA	Linear Discriminant Analysis
LoG	Laplacian of Gaussioan
LPQ	Local Phase Quantisation
MRF	Markov Random Fields
MWIR	Middle Wave Infra-Red

NIR	Near Infra-Red
PCA	Principal Component Analysis
PHOG	Pyramid of Histogram of Oriented Gradients
PPNN	Parzen Probabilistic Neural Network
ROC	Receiver Operating Characteristic
ROI	Region Of Interest
SIFT	Scale Invariant Feature Transform
SSR	Single Scale Retinex
STFT	Short Term Fourier Transform
SURF	Speeded Up Robust Features
SWIR	Short Wave Infra-Red
VIS	Visible light

Chapter 1

Introduction

1.1 Overview

Periocular region corresponds to the region of the eye as well as the area surrounding it. This can be easily acquired at the time of face or iris image acquisition. In addition to civilian applications, it plays an indispensable role in surveillance applications that aid law enforcement agencies. For example, in establishing the identity of an offender wearing a ski-mask, whose facial images have been captured by a surveillance camera. As discussed in [1], a user may also cover his face partially for health related reasons. It is known that face recognition algorithms perform poorly in presence of such occlusions. But performance of periocular recognition does not depend on these occlusions. Also this region is invariant to variations in facial expression.

Iris recognition is used in India and United Arab in their Aadhaar Program and border security programs, respectively [2]. It has also been shown [3] that the challenges that iris recognition faces in unconstrained scenarios can be overcome by adopting periocular biometrics. The recognition performance of iris biometrics is better for the case of NIR images whereas periocular biometrics performs satisfactorily in both VIS and NIR spectra. In addition, this region has high discriminating ability and are relatively permanent [4]. Therefore, the periocular region is regarded as an important biometric

trait.

Traditional biometric systems rely on intra-spectral data where both the enrolled and query images are of the same spectrum. However, advanced surveillance applications need Infra-red (IR) sensors to be installed into the system to have a clear visualization of offenders during night time. However, existing databases mostly include VIS gallery images. Therefore, development of algorithms that can match VIS-IR images is highly required.

Cross-spectral face recognition systems have gained importance in the last two decades due to their high impact in the field of practical security applications. Many researchers have put their efforts for developing cross-spectral matching systems that deal with NIR, short wave infra-red (SWIR), middle wave infra-red (MWIR) and VIS spectrum images [5, 6].

1.2 Related work

Periocular biometrics has received a lot of attention ever since its utility as a biometric trait has been investigated by Park *et al.* [7]. The authors have investigated periocular biometrics using global and local descriptors such as LBP and scale invariant feature transform (SIFT) features. Their experiments included cropping of periocular regions from their own collected face database and recognition. The extended version of their work can be found in [8].

In recent years, several approaches have been developed for periocular recognition. Authors in [9] have performed periocular recognition using convolutional restricted Boltzman machine(CRBM) feature based learning. In [10], the authors have investigated the performance of periocular recognition in presence of several degradation factors and also proposed a new method for extracting the region-of interest (ROI) of the periocular images. Alonso *et al.* [11] have performed NIR and VIS light periocular recognition using a new eye detection system and Gabor features. Uzair *et al.* [12] have extensively studied periocular region based person identification using videos in VIS,

NIR and hyper-spectral scenarios.

In [13], a method based on periocular skin texture for person identification is presented. The authors have performed both verification and identification experiments using LBP features and city-block similarity measure. Woodard *et al.* [14] have performed experiments to evaluate the application of periocular appearance cues for biometric identification. Mahalingam *et al.* [15] have proposed a method for periocular recognition based on LBP features on challenging datasets. Their experimental results indicate that LBP operator gives higher perfomance as compared to other feature vectors. A similar work by Xu *et al.* [16] performs a detailed investigation of a number of features that can be extracted from periocular region and compared their performances with the proposed local Walsh-transform binary pattern encoding scheme. Karahan *et al.* [17] have performed periocular region based identification using popular feature extraction algorithms such as SIFT and speeded up robust features (SURF) and showed that their method provides lower error rates than the current state-of-the-art methods.

Authors in [18] have explored projection based methods such as principal component analysis (PCA) and linear discriminant analysis (LDA) in order to perform periocular identity verification. Alonso *et al.* [19] have explored the problem of periocular recognition using retinotropic sampling grids and Gabor based decomposition of local power spectrum of the images. Mikaelyan *et al.* [20] have presented periocular recognition based on local symmetry patterns. Their feature extraction method describes neighbourhoods around the key points by projecting them onto the harmonic functions and estimates the presence of symmetric curve families around those points. The authors in [21] have proposed a method for periocular recognition which fuses LPQ and Gabor wavelet features, which not only improves the performance but also achieves robustness. Similarly Joshi *et al.* [22] have performed both verification and identification of periocular images using the features extracted from a bank of Gabor filters. They have used direct linear discriminant analysis (DLDA) method and Parzen probabilistic neural network (PPNN) for dimension reduction and classification of the feature vectors,

respectively.

A detailed survey on periocular biometrics can be found in [23]. This paper describes databases, algorithms, applications and challenges in this area. Uzair *et al.* [24] have performed periocular region based identification using NIR image sets. Hollingsworth *et al.* [25] have conducted an experiment to study the performance of humans in comparing periocular image pairs which included both NIR and VIS images. They have also calculated the performance of three different computer algorithms and compared the above results with those of human experiments.

Authors in recent years have also focused on combining both iris and periocular biometrics. This not only improves the performance of individual traits but also accounts for eliminating their drawbacks. In [26], different iris and periocular matchers are fused in both VIS and NIR spectra. Authors have also compared both iris and periocular biometrics based on their recognition accuracies. Santos *et al.* [27] have proposed a method to improve cross-sensor iris recognition problem by combining both iris and periocular images through score level fusion. Authors in [28] have also performed combination of iris and periocular biometrics in the visible spectrum using weighted sum rule and showed that the performance of the combination is higher than those of individual biometrics. Raja *et al.* [29] have explored iris and periocular recognition problem in the visible spectrum using binarized statistical image features (BSIF) and independent component analysis (ICA). In [30], the authors have performed fusion of iris and periocular biometrics in NIR spectrum and showed that in case of non-ideal imagery, the fusion outperforms the iris biometrics. Tan *et al.* [31] have proposed an automatic joint iris and periocular recognition at-a-distance using Leung-Mallik filter based features. Their experiments show an improvement of rank-1 identification rate over only that of iris recognition.

Another application of periocular biometrics is for soft biometric classification, such as gender recognition. Lyle *et al.* [32] have investigated the performance of local appearance based features extracted from periocular images in VIS spectrum for soft

classification on gender and ethnicity . They have also extended their work in [33] where gender classification is performed both in VIS and NIR spectra. Authors in [34] have performed periocular region based gender recognition for gender transformation cases and showed that periocular region outperforms the face component based method.

Existing studies in periocular biometrics have focused largely on intra-spectral matching. However, advanced surveillance applications require cross-spectral matching of periocular images, especially, matching query NIR images with VIS images in the gallery and vice-versa. The problem of cross-spectral matching has been studied in the context of face [5, 35, 36] and iris [37–39] biometrics. Xu *et al.* [5] have proposed a joint dictionary learning and reconstruction based method for matching face images across NIR and VIS spectra. Maeng *et al.* [35] have included cross-spectral face recognition with short and long distance measures. Zhu *et al.* [36] have addressed the problem of cross-spectral matching of NIR and VIS face images using transduction method. They have also proposed a feature representation to alleviate the heterogeneities between the VIS and NIR images. In [37], the authors have examined the possibility of cross-domain iris matching. They have also analyzed iris imaging at longer wavelengths. Zuo *et al.* [38] presented an adaptive method to match the NIR iris images against color iris images. In [39], both sensor-specific and wavelength-specific cross-matching of iris images based on domain adaption framework are proposed.

Recently, there have been some efforts to address the matching of periocular images in cross-spectral scenarios [1, 40–43]. Sharma *et al.* [40] have presented a neural network based approach, which uses pyramid of histogram of oriented gradients (PHOG) features. In their approach, two neural networks are trained separately for VIS and NIR spectra and then combined to train on the cross-spectral features. Their approach achieves genuine acceptance rate (GAR) of 47.08% at 1% false acceptance rate (FAR).

The approach presented in [41] involves Gabor filtering, followed by feature extraction and encoding. The I-divergence distance measure is used for comparing feature vectors. The performance evaluation has been carried out using their in-house database,

which contains images acquired at short as well as long standoff distances. Authors have also explored cross-spectral matching of SWIR and MWIR images. Results from their extended study is presented in [42] and [43].

Ramaiah and Kumar [1] have presented an approach for cross-spectral periocular recognition based on markov random fields (MRF) and variants of LBP. Authors have also shown that performance of periocular matching can be improved further by using real-valued features extracted from iris regions. They have reported GARs of 73.20% and 18.35% at 0.1 FAR on PolyU and IMP databases, respectively.

It is evident from the discussion here that the performance of periocular biometrics in cross-spectral scenarios needs to be improved significantly before these algorithms can be deployed in real-world applications. This motivated us to develop an approach for accurate periocular recognition in cross-spectral scenarios.

1.3 Organization of the thesis

The thesis is organized as follows:

- In Chapter 2, the proposed periocular recognition approach is discussed. The first section describes in detail different processing stages involved in the proposed method for cross-spectral matching of periocular images. Section 2 includes a detailed description of the databases used. Details of the in-house cross-spectral periocular database is given in section 3.

- In Chapter 3, experimental results for both verification and identification experiments are presented on all four databases. This also includes a brief discussion of the performance results.

- In Chapter 4, conclusions are made and a discussion on the possibility of future work is presented.

Chapter 2

Proposed Periocular Recognition Based on Illumination Normalisation

2.1 Proposed method

The core of our approach for cross-spectral periocular recognition is the DoG filtering for illumination normalization. Figure 2.1 shows the block diagram of our approach for both verification and identification scenarios, which consists of three processing stages namely, pre-processing, feature extraction and matching.

2.1.1 Pre-processing

In the proposed approach, the inherent illumination variation between the VIS and the NIR images is handled at the pre-processing stage. Specifically, images are convolved with a DoG filter to mitigate the illumination variations, which adversely affect the matching of VIS and NIR periocular images. This process generates images that are largely free of illumination induced variations.

Essentially, DoG is a band-pass filter which has been shown to approximate the

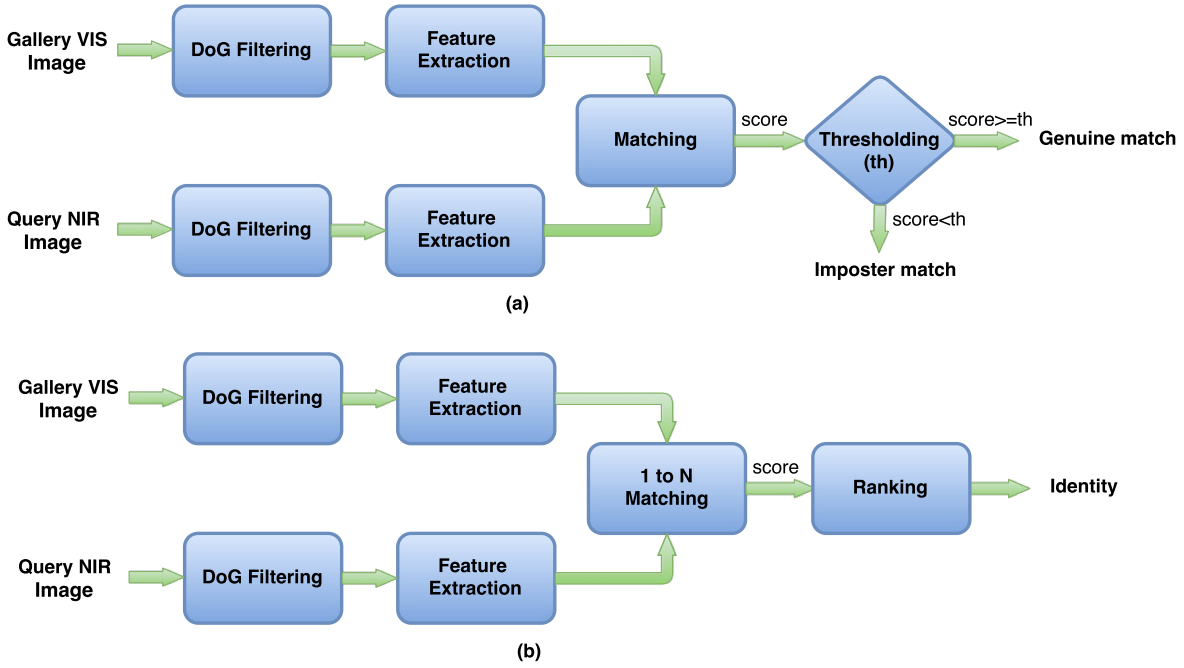

Figure 2.1: Block diagram of the proposed method: (a) Verification scenario, (b) Identification scenario

Laplacian of Gaussian (LoG) function. The Laplacian operator and the Gaussian function are defined as follows:

$$\nabla^2 = \frac{\delta^2}{\delta x^2} + \frac{\delta^2}{\delta y^2} \tag{2.1}$$

and

$$G(x, y) = exp(-\frac{x^2 + y^2}{2\sigma^2}) \tag{2.2}$$

The LoG function is then defined as follows:

$$\nabla^2 G(x, y) = \frac{x^2 + y^2 - 2\sigma^2}{\sigma^4} exp(-\frac{x^2 + y^2}{2\sigma^2}) \tag{2.3}$$

In the above equation, the Gaussian part blurs the image, reducing structural noises at scales much smaller than the standard deviation σ. Unlike averaging masks, Gaussian operator is smooth in both spatial domain and frequency domain. Therefore, less artifacts are introduced. The Laplacian part is isotropic and hence invariant to rotation

which also corresponds to its in-variance to changes in intensity in any direction.

For an image $I(x, y)$, DoG filtering can be mathematically expressed as follows:

$$DoG * I(x, y) = (G_{\sigma_1} - G_{\sigma_2}) * I(x, y) \tag{2.4}$$

$$= G_{\sigma_1} * I(x, y) - G_{\sigma_2} * I(x, y) \tag{2.5}$$

where G_{σ_1} and G_{σ_2} are the discrete Gaussian kernels having standard deviation σ_1 and σ_2, respectively. We have used σ_1 and σ_2 as 1 and 2 respectively. The symbol $*$ represents the two-dimensional convolution operation. In general, a Gaussian kernel can be defined as follows:

$$G_\sigma(x, y) = \frac{1}{\sqrt{2\pi}\sigma} exp(-\frac{x^2 + y^2}{2\sigma^2}) \tag{2.6}$$

Figures 2.2, 2.3 and 2.4 show the results of illumination normalization using DoG filtering on sample VIS and NIR images from IMP, PolyU and cross-eyed databases respectively. As can be observed, the resultant images look very similar in all the three cases.

2.1.2 Feature extraction and matching

Having performed the illumination normalization, we have extracted texture and shape descriptors that carry discriminatory information useful for matching the query NIR image to the enrolled VIS images of the claimed identity. Specifically, we have explored four popular feature descriptors namely, LBP, HOG, Gabor and LPQ features for this purpose.

LBP is a texture descriptor that has been successfully applied to diverse image analysis tasks. We have used $LBP_{1,8}$ [44] features computed using a circular neighbourhood of unit radius with eight sampling points. Considering uniform binary patterns, the above process generates a 59-dimensional histogram feature.

HOG features effectively capture local shape information and have been shown to outperform wavelets and other gradient based descriptors [45].

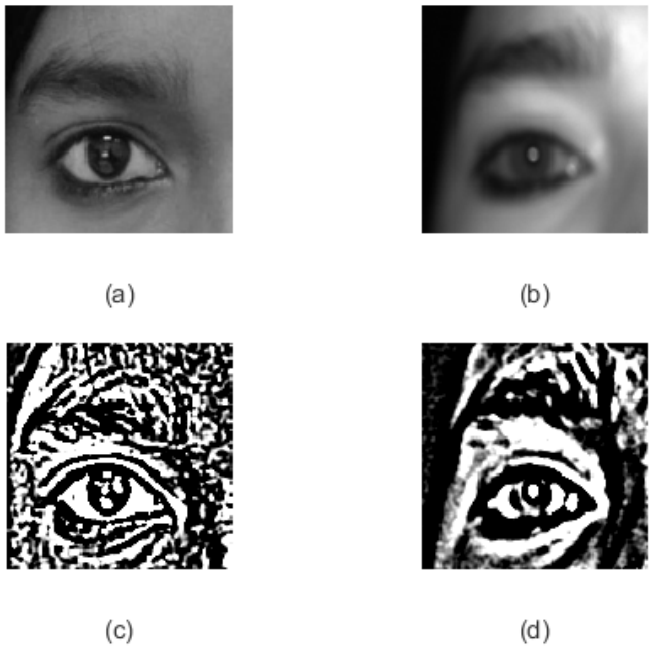

Figure 2.2: Illustration of DoG filtering on IMP database: (a) VIS periocular image, (b) NIR periocular image, (c) DoG filtered VIS periocular image and (d) DoG filtered NIR periocular image

The LPQ [46] is a blur insensitive texture classification method, which uses local phase information extracted using short-term Fourier transform (STFT) computed in local neighborhood at each pixel position of the image.

We have also used Gabor filter based features in our experiments where the magnitudes of the filtered image at each pixel are considered as features [47]. This feature is insensitive to changes in rotation, scale, translation, illumination and noise.

The proposed approach uses the COS metric for comparison of the feature vectors extracted from the query and the enrolled images. Suppose $\mathbf{p} = (p_1, p_2, ..., p_n)$ and $\mathbf{q} = (q_1, q_2, ..., q_n)$ denote the two n-dimensional feature vectors being compared. The COS score, which provides a measure of similarity between the two vectors $\mathbf{p}$ and $\mathbf{q}$, is

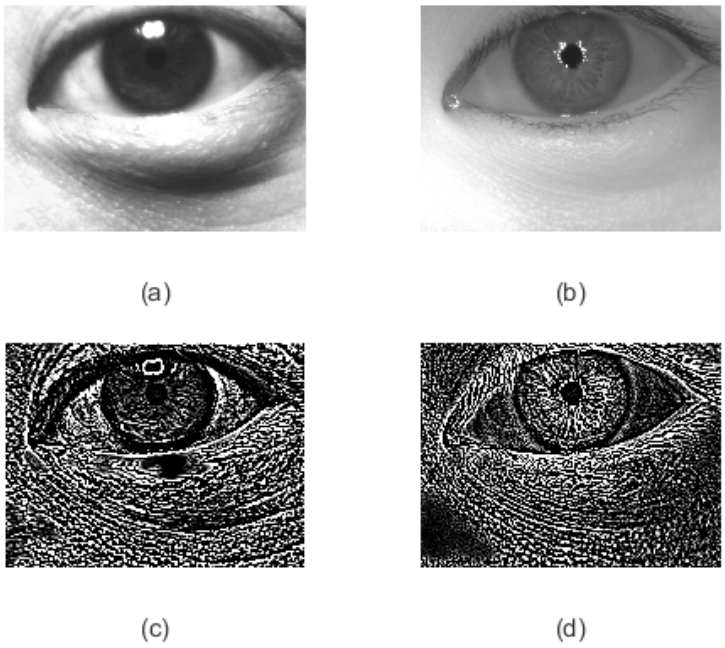

Figure 2.3: Illustration of DoG filtering on PolyU database: (a) VIS periocular image, (b) NIR periocular image, (c) DoG filtered VIS periocular image and (d) DoG filtered NIR periocular image

defined as follows:

$$D(\mathbf{p}, \mathbf{q}) = \frac{\mathbf{p} \cdot \mathbf{q}}{\|\mathbf{p}\|\|\mathbf{q}\|} \tag{2.7}$$

$$= \frac{\sum_{i=1}^{n} p_i q_i}{\sum_{i=1}^{n} \sqrt{p_i^2} \sum_{i=1}^{n} \sqrt{q_i^2}} \tag{2.8}$$

2.2 Databases and experimental protocol

Performance of the proposed approach has been evaluated on three publicly available periocular image databases namely, IMP periocular dataset, PolyU iris database and cross-eyed periocular database. The following section presents detailed descriptions of the databases and the experimental protocol adopted for performance evaluation for both verification and identification scenarios.

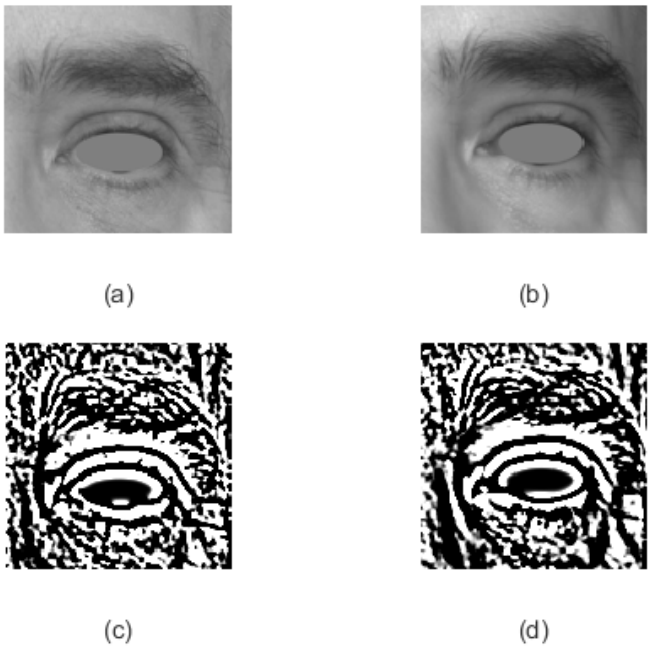

Figure 2.4: Illustration of DoG filtering on cross-eyed database: (a) VIS periocular image, (b) NIR periocular image, (c) DoG filtered VIS periocular image and (d) DoG filtered NIR periocular image

1. **IMP database**

   This database contains periocular images of 62 subjects, with 5 images each captured in VIS, NIR and night vision spectra. In this work, we have used periocular images captured only in the VIS and NIR spectra. Figure 2.5 shows sample VIS and NIR periocular images of a subject in this database.

   As can be seen in this figure, the VIS images in the database contain both left and right periocular regions and each of these images has a dimension of 301×601 pixels. Therefore, we have separated each of the VIS images into left and and right periocular images. Before separating the left and right periocular images, we have performed eye-pair detection using Viola-Jones algorithm [48]. Once an eye-pair is detected, a rectangular ROI around the eye is extracted. The ROI

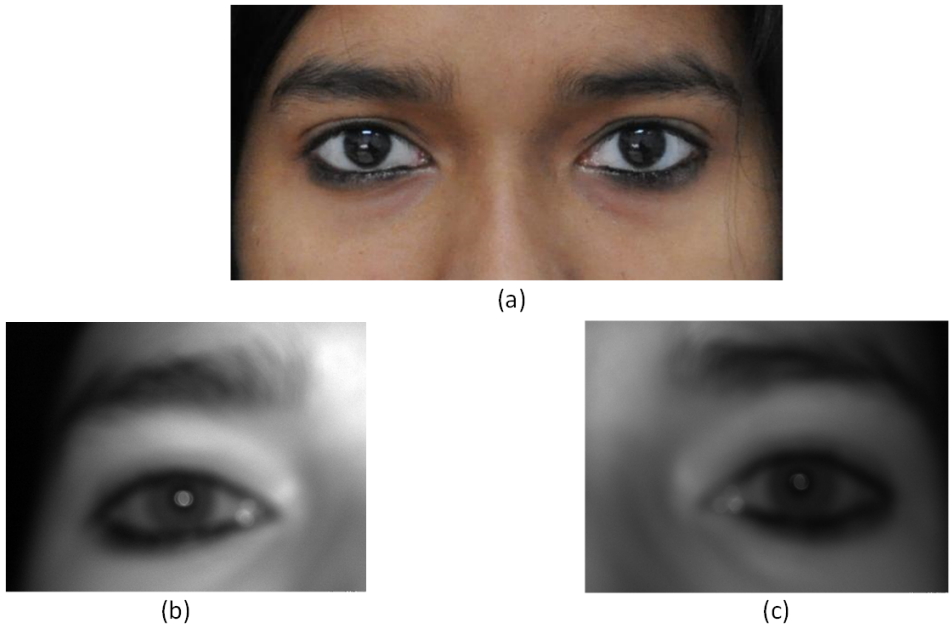

Figure 2.5: Sample images from IMP database: (a) VIS periocular image (b) left and (c) right NIR periocular images

size is determined based on the dimensions of the bounding box produced by the eye-pair detector. Specifically, it is $(w + \frac{w}{a}, h + \frac{h}{b})$ pixels, where w and h are the width and the height of the bounding box, respectively. The parameters a and b in the fractions are set empirically in our experiments.

On the other hand, NIR images of the left and right periocular regions have been captured separately, with each containing 640×480 pixels. Therefore, a total of 1240 left and right periocular images, with 620 images each in the VIS and NIR image subsets, have been used in our experiments. To reduce computation time, we have down-sampled these images to 64×64 pixels.

2. **PolyU cross-spectral iris database**

The PolyU cross-spectral iris database [39] contains VIS and NIR periocular images from 209 subjects with 15 images per spectrum per subject. There are separate images for left and right periocular regions. Figure 2.6 shows the sample

periocular images. The original images have dimensions of 640×480. We have down-sampled these periocular images to 60×80 pixels for further processing.

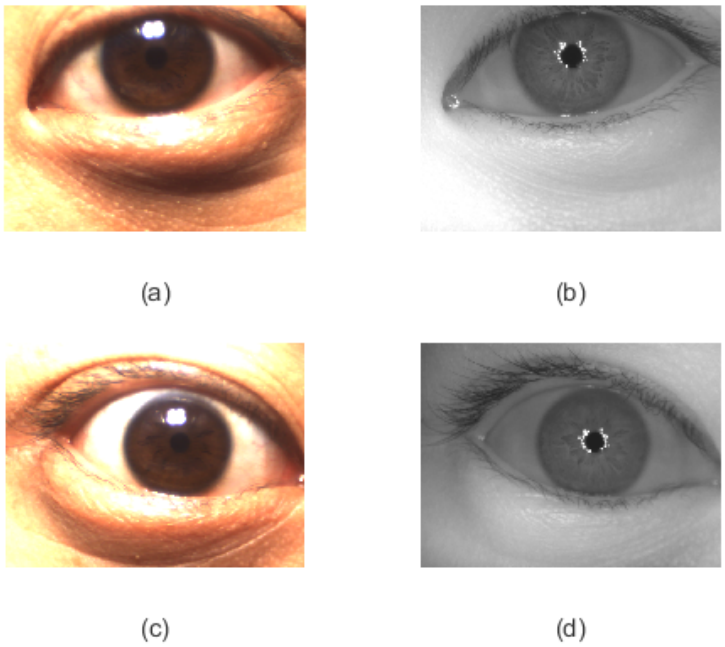

Figure 2.6: Sample images from PolyU cross-spectral iris database: (a) Left VIS periocular image (b) Left NIR periocular image (c) Right VIS periocular image and (d) Right NIR periocular image

3. **Cross-eyed periocular database**

   The cross-eyed periocular database [49] contains 8 VIS and NIR images of both left and right periocular regions for each of the 120 subjects. Figure 2.7 shows the sample VIS and NIR images for left and right periocular regions of a subject in this database. In the database, the eye regions are masked so as to avoid use of iris information. The original size of each of the periocular images is 800×900 pixels. We have down-sampled each of them into 64×64 pixels.

Table 2.1 shows an overview of the three periocular databases used in our experiments.

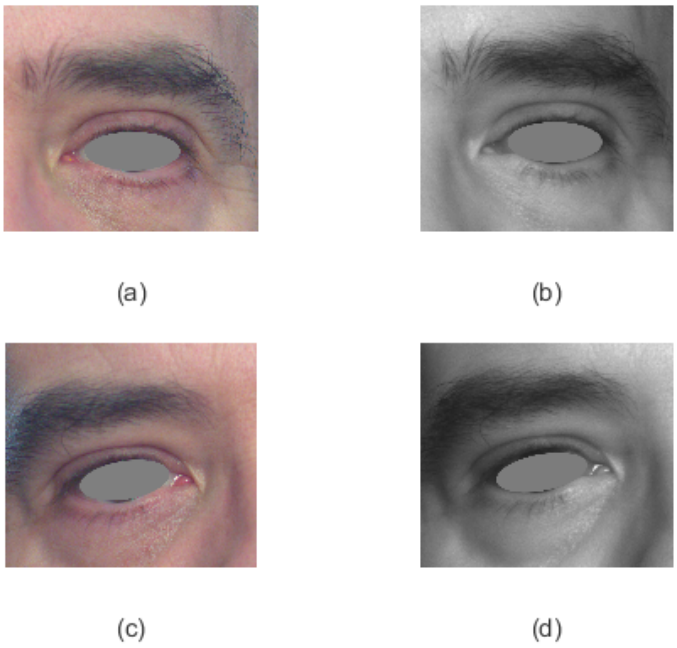

Figure 2.7: Sample images from Cross-eyed database: (a) Left VIS periocular image (b) Left NIR periocular image (c) Right VIS periocular image and (d) Right NIR periocular image

2.3 Development of a new cross-spectral periocular database

Though cross-spectral periocular biometrics has been extensively researched upon, only a few number of databases are available publicly, on which the performance can be evaluated. This motivated us to develop a new and challenging cross-spectral periocular database. Our database consists of images from 201 subjects (144 males and 57 females), most of which are students of IIT Indore. The database has been collected in three different sessions (July 2016, December 2016 and May 2017). These images are captured in both NIR and VIS spectra and at two different stand-off distances with 7 different pose variations. Hence, a total of 5628 images from 201 subjects are collected.

The dataset is created using HIK Vision IR cube network camera, which is a true

Table 2.1: Overview of the databases used

Database / Properties	IMP database	PolyU database	Cross-eyed database
Development	IIIT Delhi (2014)	Hong Kong Polytechnic University (2014)	University of Reading, USA (2016)
Subjects	62	209	120
Spectra	VIS NIR Night Vision	VIS NIR	VIS NIR
No of images per subject per spectra	5	15	8
Size of images	301-by-601 (VIS) 640-by-480 (NIR)	480-by-640	800-by-900

day and night camera. The sensor present in the camera detects the presence of light and thus automatically switches the mode of operation between VIS and NIR. Network camera is a small and reliable embedded digital surveillance product with combined features of both traditional analog camera and network digital video server (DVS). This camera finds its application in remote control network applications such as network surveillance for markets and industries as well as remote surveillance for homes and offices.

Initially, we have captured streams of videos of each individual which includes continuous variations in pose. The frames are then extracted from those videos with required pose variations at different instants of time. The next task is to crop the periocular regions from the whole images. To accomplish this task, we have performed eye-pair detection using Viola-Jones algorithm [48]. This algorithm crops the periocular regions by using the previously cropped face regions. Figure 2.8 shows the images corresponding

to the input and output of this process.

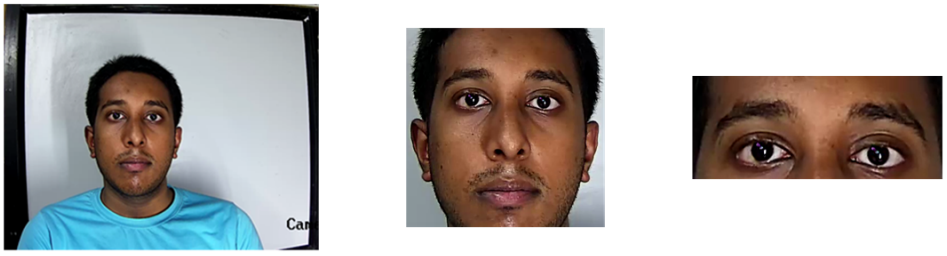

Figure 2.8: (a) Original image extracted from the captured video stream, (b) Cropped face image, (c) Cropped periocular image

Finally all the images are resized to dimensions of 60×120 pixels. As can be seen from Figure 2.8, the cropped images contain left and right periocular images. Hence we have separated the left and right periocular images while performing individual experiments. This results in left and right periocular images of dimension 60×60 pixels. Table 2.2 shows the properties of the database created.

Figures 2.9, 2.10, 2.11 and 2.12 show the sample images corresponding to VIS and NIR periocular images of a male subject and a female subject, respectively. As we can see from these figures, the images correspond to the pose variations indicated in Table 2.2.

The performance evaluation on this database has been partitioned into two different sets of experiments. The first set of experiments are performed on a subset of the in-house dataset which contains first 5 images (corresponding to eye movement only) from all subjects, resulting in a total of 4020 images. The second set of experiments are performed on the entire database. These two sets of images have been named as image sets 1 and 2 respectively. The motivation of performing two sets of experiments can be well explained if we will look at Figures 2.9 to 2.12. From these figures, it can be seen

Table 2.2: Properties of the new cross-spectral periocular database

Development	By IIT Indore	
Subject description	201 subjects 144 males and 57 females	
Number of images	7 images per subject per spectrum per distance measure	
Variations	Spectra	VIS
		NIR
	Distance	Near distance (0.3 m)
		Far distance (0.9 m)
	Pose	Eye movement (Front, Left, Right, Up, Down)
		Face movement (Left, Right)

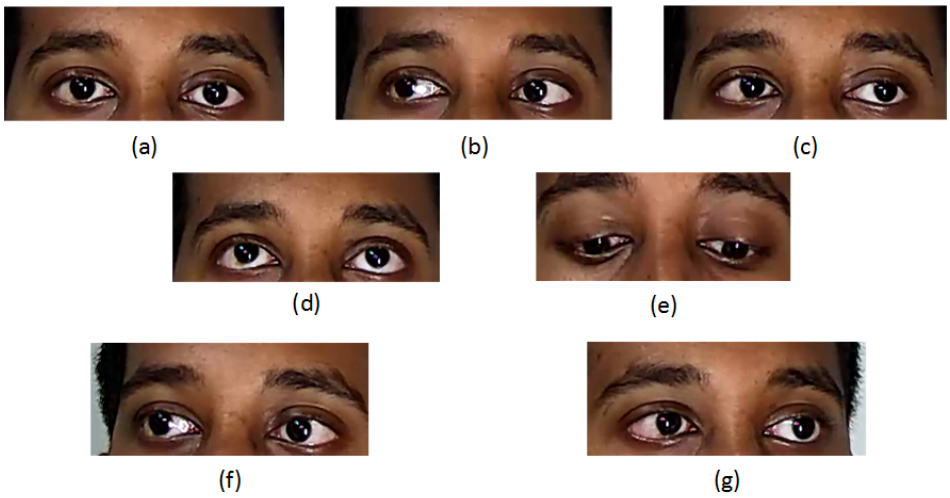

Figure 2.9: VIS periocular images corresponding to a male subject

that images corresponding to face movement contain background regions in addition to the periocular regions. This is because, the position of the camera does not change

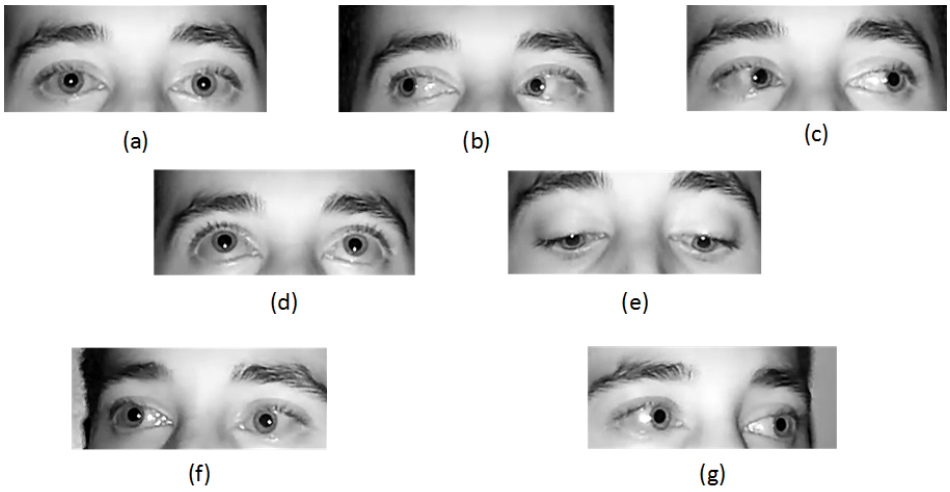

Figure 2.10: NIR periocular images corresponding to a male subject

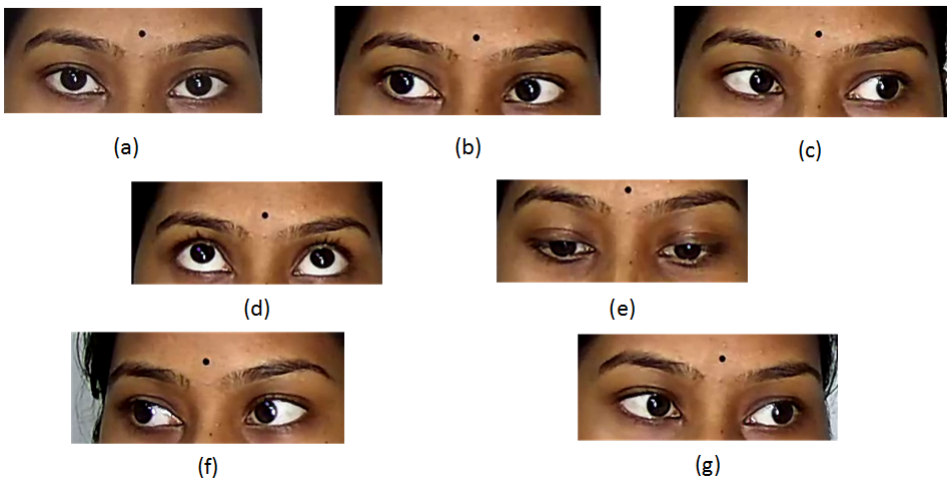

Figure 2.11: VIS periocular images corresponding to a female subject

with respect to the face. Due to this, the performance on the overall database degrades slightly. On the other hand, this makes the database more challenging from practical point of view.

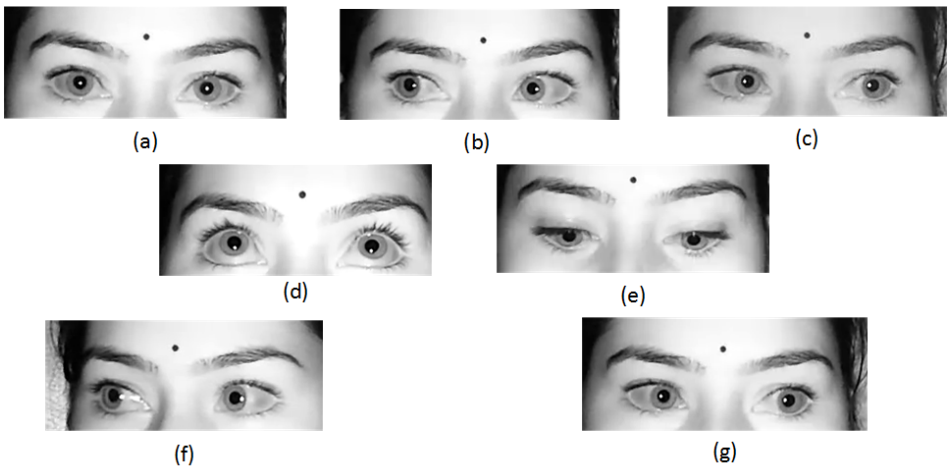

Figure 2.12: NIR periocular images corresponding to a female subject

Chapter 3

Experiments and Discussion

In order to evaluate the performance of the proposed approach, we have performed verification as well as identification experiments. For the case of verification experiments, in addition to the receiver operating characteristic (ROC) curves, we report the equal error rates (EER) and GARs at 0.1 FAR as the performance measures. Similarly, the performance measures in case of identification experiments include the rank-1 and rank-10 recognition rates and cumulative match characteristic (CMC) curves.

3.1 Verification experiments

In this section, we present results from a set of verification experiments that have been carried out to evaluate the performance of our approach using left and right periocular images. We have also evaluated the performance of our approach when the left and right periocular images are combined at the feature-level through simple feature concatenation.

Tables 3.1, 3.2 and 3.3 present results from our experiments on IMP, PolyU and cross-eyed databases, respectively. As mentioned previously, these tables show EERs (%) and GARs (%) at 0.1 FAR for verification using the left periocular images, right periocular images and their feature-level combination.

As can be seen from Table 3.1, the LPQ feature yields higher GARs (%) for the

Table 3.1: Verification performance of the proposed method on IMP database

Features	Left Periocular		Right Periocular		Combined	
	EER (%)	GAR (%)	EER (%)	GAR (%)	EER (%)	GAR (%)
LBP	45.34	10.19	45.82	9.87	45.29	10.19
HOG	43.85	23.81	46.01	**24.97**	45.84	25.03
Gabor	41.41	24.90	45.01	19.55	41.19	23.74
LPQ	38.76	**30.00**	39.46	23.94	37.83	**32.06**

Table 3.2: Verification performance of the proposed method on PolyU database

Features	Left Periocular		Right Periocular		Combined	
	EER (%)	GAR (%)	EER (%)	GAR (%)	EER (%)	GAR (%)
LBP	36.61	25.56	35.74	29.43	33.55	35.37
HOG	19.57	**70.97**	18.79	**73.12**	13.87	**83.12**
Gabor	22.95	61.01	22.84	62.87	17.27	75.41
LPQ	27.16	44.06	24.91	52.14	19.81	66.13

IMP database. However for the case of right periocular images, both HOG and LPQ features perform similarly. Table 3.2 shows that for PolyU database the performance of HOG feature is significantly higher for left, right and combined periocular images. Similarly, from Table 3.3 we can see that, the LPQ feature yields higher GAR (%) values for cross-eyed database.

The results presented in these tables clearly indicate that the HOG and LPQ descriptors yield consistently higher GARs for left,right as well as combined periocular matching. This is indicated in boldface in the tables. The superior performance of the HOG and LPQ features as compared with LBP and Gabor features is perhaps due to

Table 3.3: Verification performance of the proposed method on Cross-eyed database

Features	Left Periocular		Right Periocular		Combined	
	EER (%)	GAR (%)	EER (%)	GAR (%)	EER (%)	GAR (%)
LBP	17.62	69.39	15.11	76.65	10.36	89.27
HOG	16.55	80.03	17.63	77.55	13.22	85.35
Gabor	14.02	83.49	16.04	80.29	11.27	88.01
LPQ	6.68	**94.51**	5.85	**95.48**	3.99	**97.14**

the fact that the normalized periocular images contain largely shape information, which these descriptors are capable of capturing effectively.

Similarly, for the in-house database, Tables 3.4 and 3.5 show EERs (%) and the verification accuracies in terms of GARs (%) at 0.1 FAR value on image sets 1 and 2, respectively.

Table 3.4: Verification performance of the proposed method on image set 1

Features	Left periocular		Right periocular		Combined	
	EER (%)	GAR (%)	EER (%)	GAR (%)	EER (%)	GAR (%)
LBP	39.24	23.24	33.99	25.47	39.54	23.05
HOG	34.28	**46.06**	32.34	**48.85**	30.73	**55.05**
Gabor	37.28	38.67	35.27	41.38	33.67	46.64
LPQ	33.24	39.63	33.99	37.84	32.92	39.34

As can be seen from these tables, performance of HOG feature descriptor is highest for all cases. We can also observe that performance of the proposed method on image

Table 3.5: Verification performance of the proposed method on image set 2

Features	Left periocular		Right periocular		Combined	
	EER (%)	GAR (%)	EER (%)	GAR (%)	EER (%)	GAR (%)
LBP	42.40	20.96	41.91	22.06	40.85	21.02
HOG	37.82	**38.94**	35.84	**41.82**	34.51	**46.37**
Gabor	39.14	35.01	37.30	36.79	35.95	41.46
LPQ	37.91	33.03	38.45	31.95	35.76	34.44

set 2 is lower than that of the image set 1 (as we have discussed in chapter 2).

Figures 3.1, 3.2 and 3.3 show the ROC curves for IMP database for VIS-NIR matching of left periocular images, right periocular images and combined periocular images, respectively.

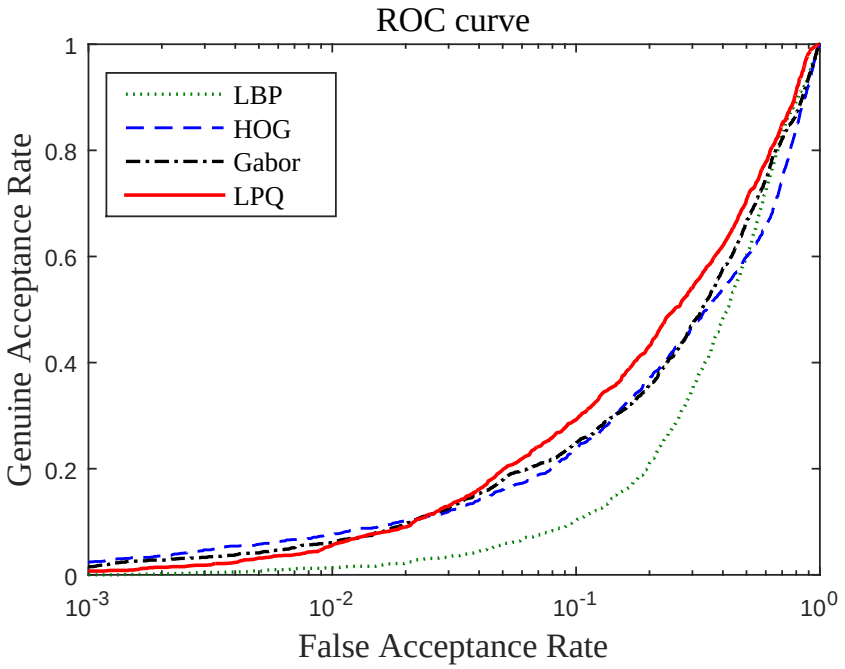

Figure 3.1: ROC curves for IMP database (Left periocular)

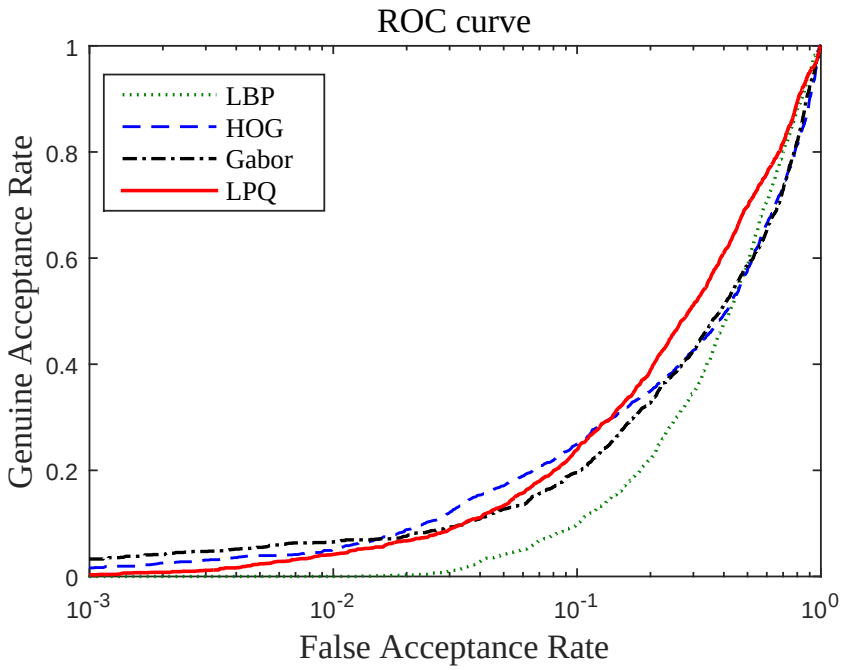

Figure 3.2: ROC curves for IMP database (Right periocular)

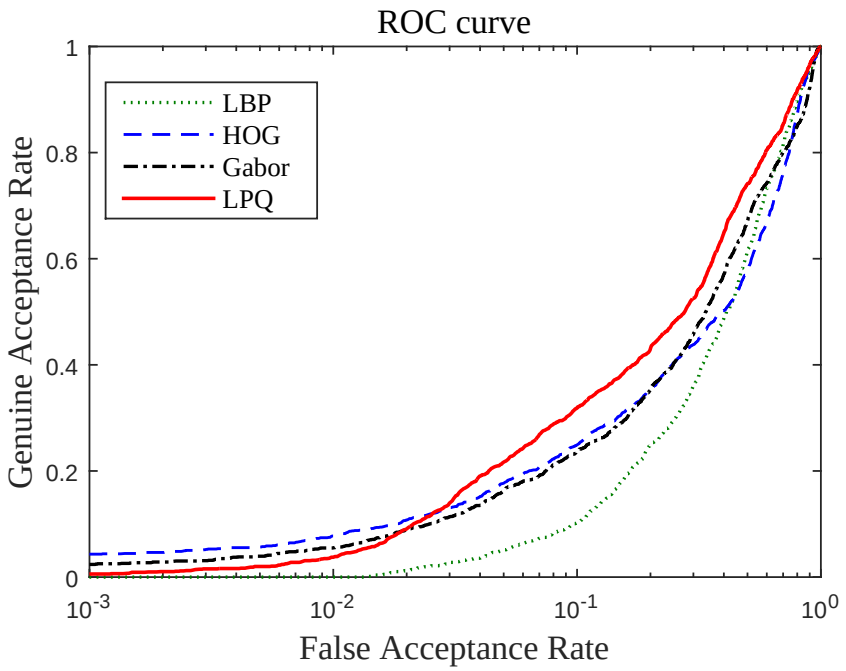

Figure 3.3: ROC curves for IMP database (Combined)

Figures 3.4, 3.5 and 3.6 show the ROC curves for PolyU database for VIS-NIR matching of left periocular images, right periocular images and combined periocular images, respectively.

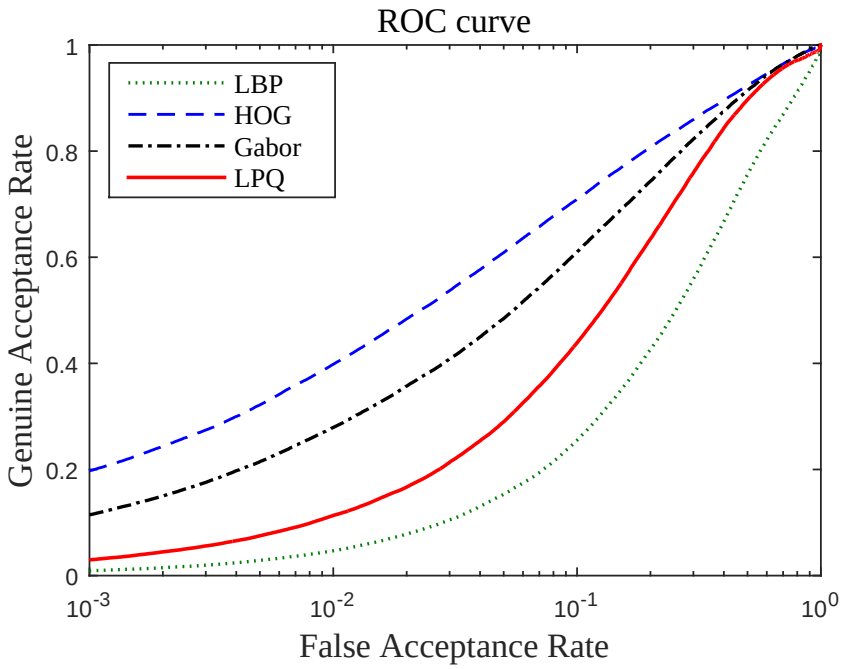

Figure 3.4: ROC curves for PolyU database (Left periocular)

Figures 3.7, 3.8 and 3.9 show the ROC curves for cross-eyed database for VIS-NIR matching of left periocular images, right periocular images and combined periocular images, respectively.

Figures 3.10, 3.11 and 3.12 show the ROC curves corresponding to VIS-NIR matching of left, right and combined periocular images belonging to image set 1.

Similarly, Figures 3.13, 3.14 and 3.15 show the ROC curves corresponding to VIS-NIR matching of left, right and combined periocular images belonging to image set 2.

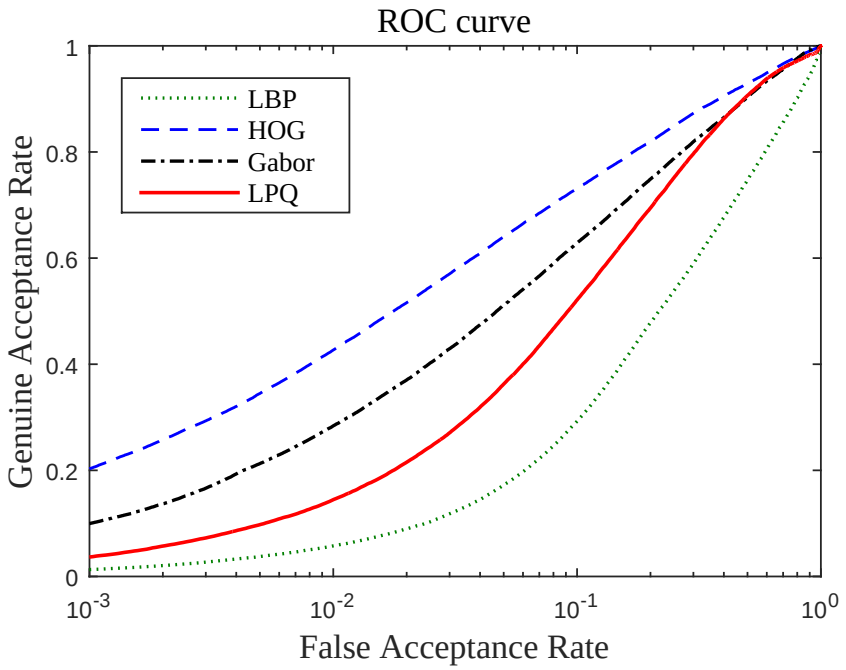

Figure 3.5: ROC curves for PolyU database (Right periocular)

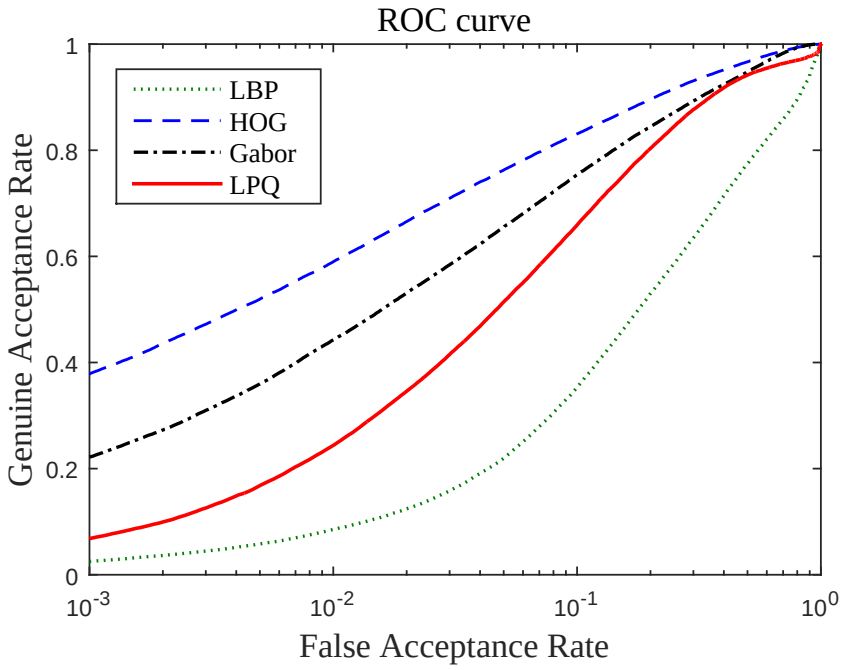

Figure 3.6: ROC curves for PolyU database (Combined)

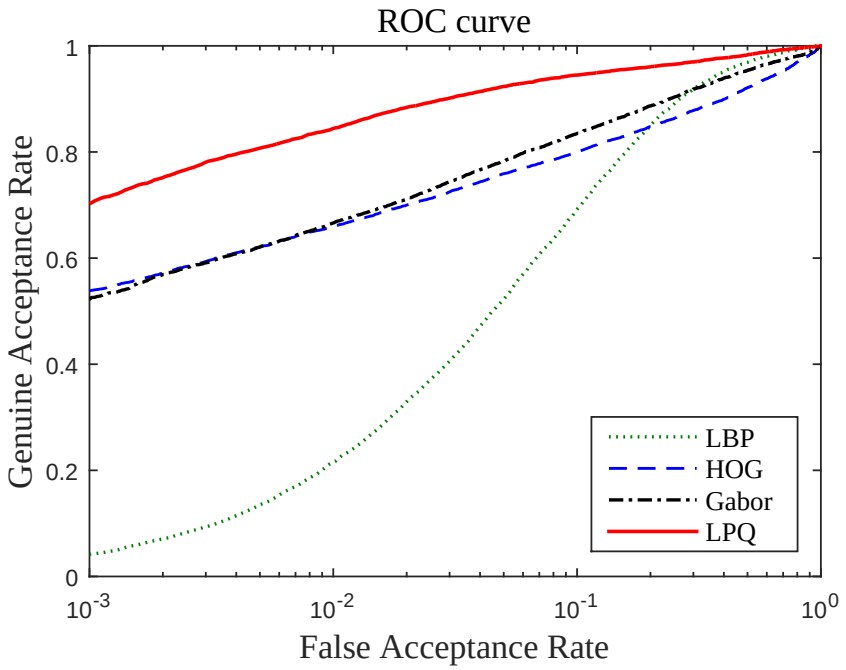

Figure 3.7: ROC curves for Cross-eyed database (Left periocular)

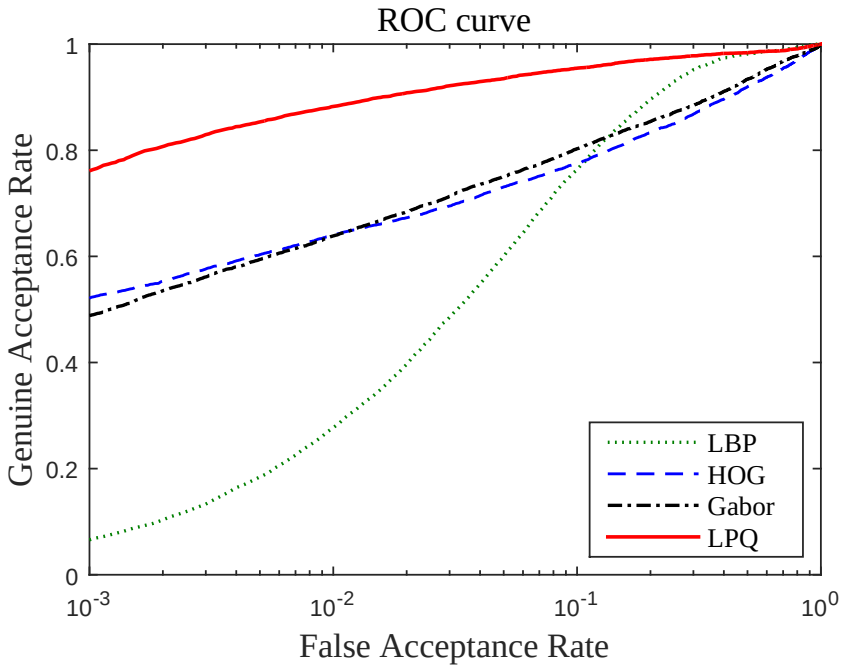

Figure 3.8: ROC curves for Cross-eyed database (Right periocular)

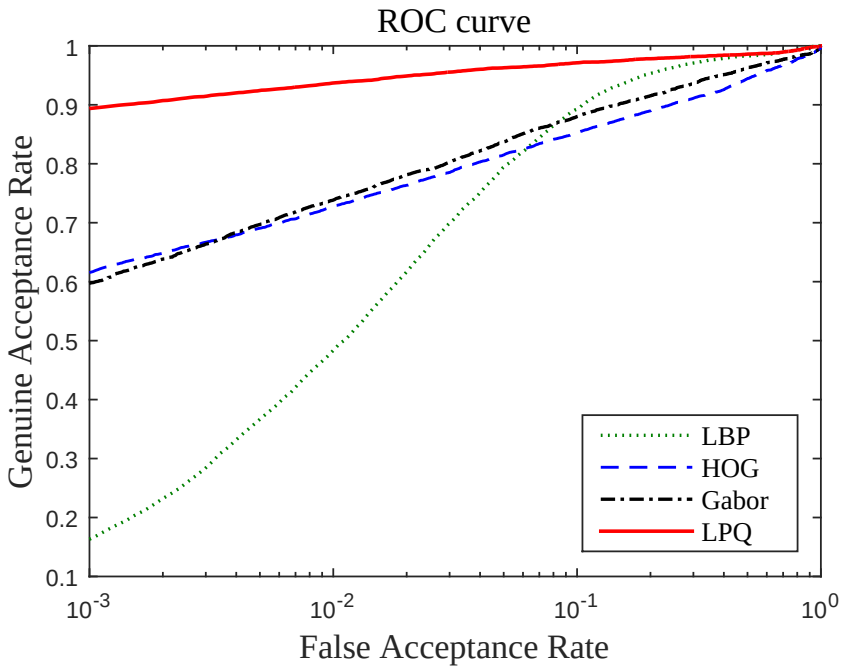

Figure 3.9: ROC curves for Cross-eyed database (Combined)

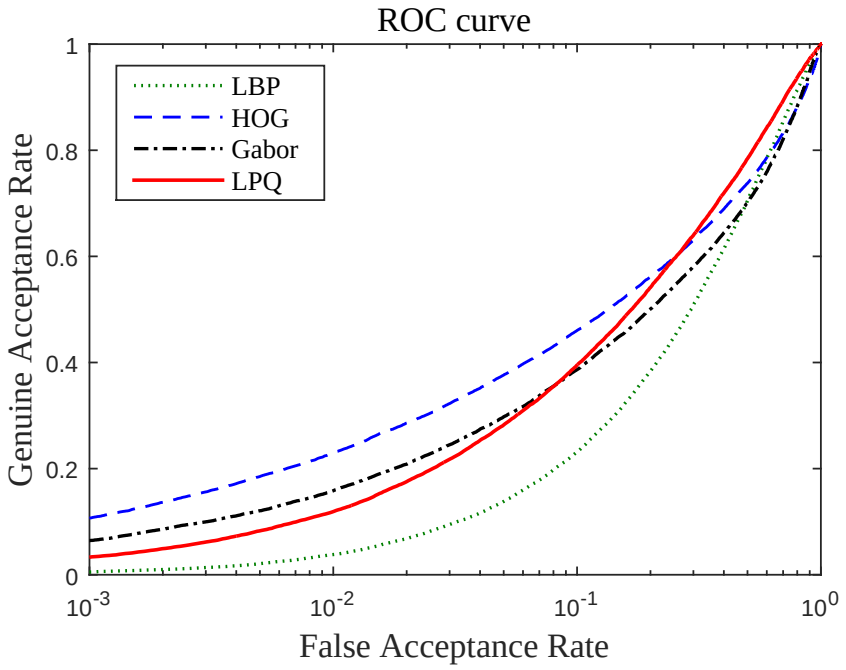

Figure 3.10: ROC curves for image set 1 (Left periocular)

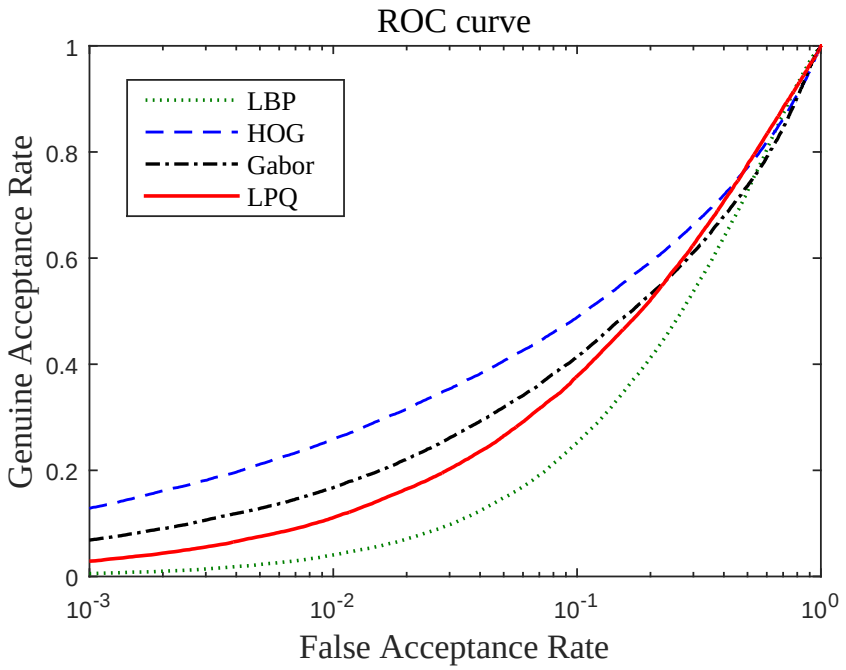

Figure 3.11: ROC curves for image set 1 (Right periocular)

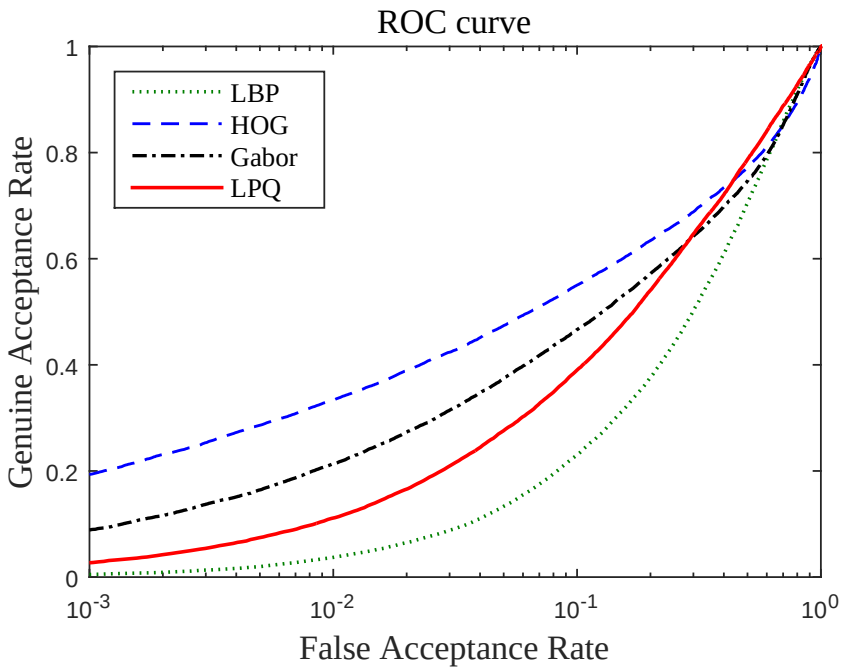

Figure 3.12: ROC curves for image set 1 (Combined)

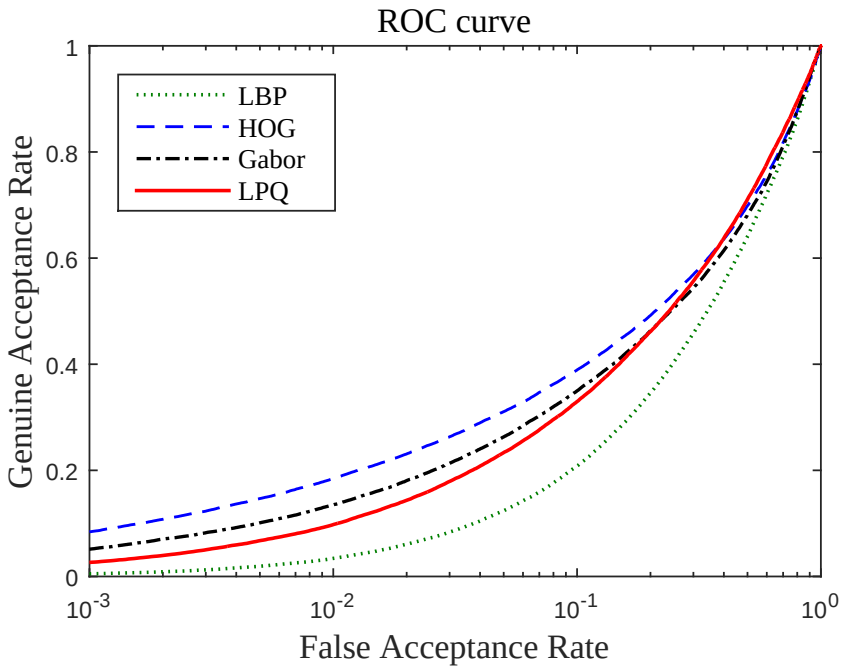

Figure 3.13: ROC curves for image set 2 (Left periocular)

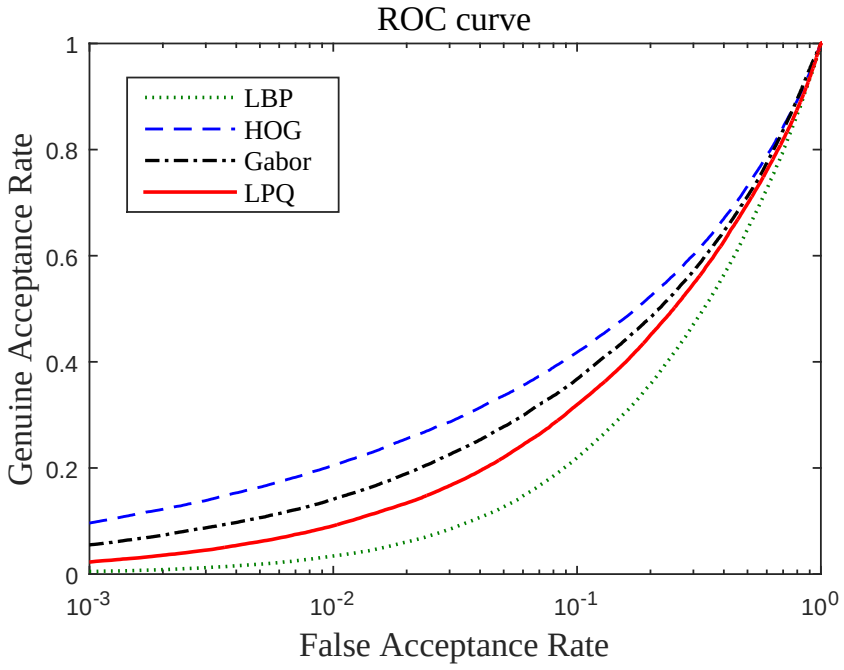

Figure 3.14: ROC curves for image set 2 (Right periocular)

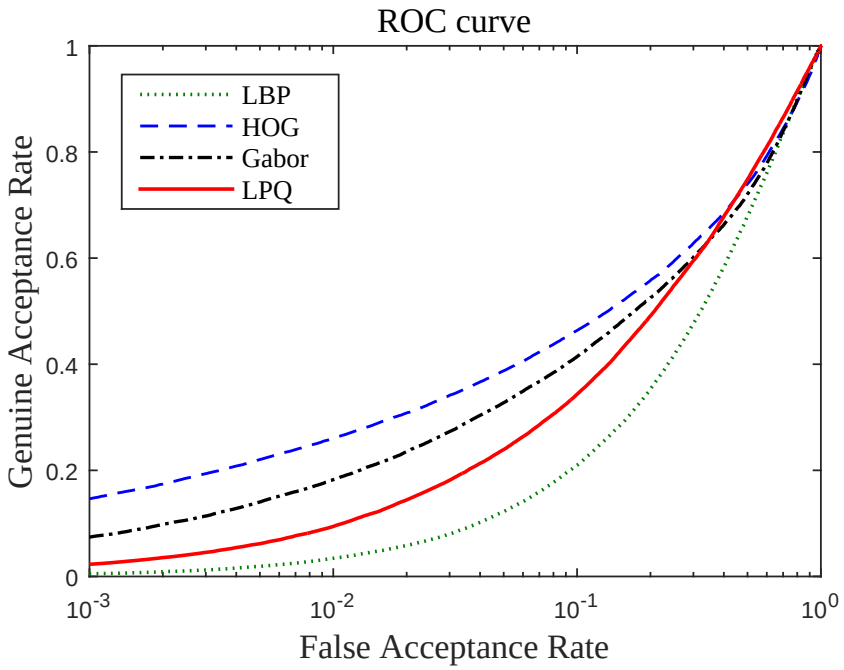

Figure 3.15: ROC curves for image set 2 (Combined)

3.1.1 Comparative analysis

For a comparison of performance, we have selected three other illumination normalization methods namely, Hilbert transform [50], contrast limited adaptive histogram equalization (CLAHE) [51] and single-scale-retinex (SSR) [52]. Table 3.6 shows the GARs (%) at 0.1 FAR for various cases. GARs (%) reported in this table correspond to the HOG feature-based approach as it has provided satisfactory performance in our previous set of experiments. As can be seen in this table, the Hilbert transform based method performs marginally better than the proposed method in a few cases, especially on the cross-eyed database. However, the performance of the proposed method is more consistent and it yields significant improvement over the Hilbert transform-based method on the PolyU database.

We have also compared the performance of our approach with the one proposed by Ramaiah *et al.* [1] as they have also evaluated their method on IMP and PolyU databases. Their approach does not require a training set of images and hence, it has

Table 3.6: Comparison of GARs (%) of various illumination normalization methods

Database \ Method		Hilbert transform	CLAHE	SSR	DoG
IMP database	Left periocular	22.52	18.58	15.48	**23.81**
	Right periocular	18.97	9.03	13.42	**24.97**
	Combined	**25.61**	15.03	16.77	25.03
PolyU database	Left periocular	55.53	65.71	50.78	**70.97**
	Right periocular	58.00	68.19	54.89	**73.12**
	Combined	68.41	76.60	58.69	**83.12**
Cross-eyed database	Left periocular	**81.72**	79.43	80.47	80.03
	Right periocular	**80.35**	77.60	77.27	77.55
	Combined	**88.31**	85.39	85.66	85.35
In-house database (Image set 1)	Left periocular	40.44	33.12	22.67	**46.06**
	Right periocular	39.95	35.24	25.19	**48.85**
	Combined	47.96	38.42	27.62	**55.05**
In-house database (Image set 2)	Left periocular	34.73	37.00	24.57	**38.94**
	Right periocular	33.90	38.96	27.23	**41.82**
	Combined	40.08	43.06	30.35	**46.37**

been evaluated on the entire dataset. Therefore, a direct comparison is made in Table 3.7 with the results reported in [1]. As can be seen, the proposed approach provides significant improvement in GAR over the existing method [1].

Table 3.7 also includes the results of Sharma *et al.* [40]. However, it may be noted that their method requires a training set of periocular images and therefore, GAR (%) is obtained on a test dataset which is a subset of the whole dataset. Therefore, a fair comparison cannot be made as our method has been evaluated on the entire database.

Table 3.7: Performance comparison with the existing approaches

Approach	IMP database	PolyU database
Ramaiah *et al.* [1]	18.35	73.20
Sharma *et al.* [40]	47.08	-
Proposed work	**25.03**	**83.12**

3.2 Identification experiments

In addition to verification experiments, we have performed identification experiments on all four databases, where the query NIR images are identified against the VIS gallery images. We present results in this case are in terms of rank-1 and rank-10 % recognition rates. We also present CMC curves for all four databases. Tables 3.8, 3.9 and 3.10 show the rank-1 and rank-10 accuracies for IMP, PolyU and cross-eyed databases, respectively.

Table 3.8: Identification performance of the proposed method on IMP database

Features	Left Periocular		Right Periocular		Combined	
	Rank 1	Rank 10	Rank 1	Rank 10	Rank 1	Rank 10
LBP	-	20.00	-	21.61	-	20.97
HOG	-	31.61	-	33.87	-	31.61
Gabor	-	25.81	-	19.68	-	25.81
LPQ	**16.45**	**54.52**	-	**45.81**	**13.55**	**55.16**

In all these tables, bold-faced numbers indicate the highest recognition rates for

Table 3.9: Identification performance of the proposed method on PolyU database

Features	Left Periocular		Right Periocular		Combined	
	Rank 1	Rank 10	Rank 1	Rank 10	Rank 1	Rank 10
LBP	-	21.91	-	24.24	-	30.72
HOG	**44.66**	**74.45**	**43.48**	**75.28**	**60.57**	**85.71**
Gabor	18.44	51.52	15.98	50.11	18.44	51.52
LPQ	12.50	39.59	17.83	49.73	27.34	68.29

Table 3.10: Identification performance of the proposed method on Cross-eyed database

Features	Left Periocular		Right Periocular		Combined	
	Rank 1	Rank 10	Rank 1	Rank 10	Rank 1	Rank 10
LBP	42.60	81.87	44.58	85.94	76.06	96.35
HOG	80.00	91.87	76.88	90.00	80.00	91.87
Gabor	53.96	80.21	51.67	78.54	53.96	80.21
LPQ	**95.83**	**98.44**	**95.21**	**98.96**	**98.54**	**99.38**

each case. LPQ feature results in highest identification accuracy for both IMP and cross-eyed database, whereas HOG feature gives consistently higher performance on PolyU dataset. Similar to verification results, LBP feature performs poorly on all the four databases.

Tables 3.11 and 3.12 show the results of the identification experiments in terms of rank-1 and rank-10 recognition rates for image sets 1 and 2, respectively.

From these tables, it can be observed that HOG performs better as compared to other features. Similar to verification experiments, proposed method has achieved better identification accuracies on image set 1 than that of image set 2.

Table 3.11: Identification performance of the proposed method on image set 1

Features	Left periocular		Right periocular		Combined	
	Rank 1	Rank 10	Rank 1	Rank 10	Rank 1	Rank 10
LBP	-	24.48	-	27.56	-	23.78
HOG	**28.81**	**54.68**	**31.09**	**57.31**	**43.88**	**66.97**
Gabor	19.20	43.53	16.82	45.02	17.36	43.68
LPQ	19.50	52.04	15.52	43.68	15.52	48.96

Table 3.12: Identification performance of the proposed method on image set 2

Features	Left periocular		Right periocular		Combined	
	Rank 1	Rank 10	Rank 1	Rank 10	Rank 1	Rank 10
LBP	-	21.57	-	23.67	-	21.75
HOG	**23.06**	**48.83**	**25.80**	**51.60**	**36.53**	**63.40**
Gabor	13.29	38.45	10.55	36.50	14.93	41.01
LPQ	14.57	43.00	12.01	37.99	12.97	43.46

Figures 3.16, 3.17 and 3.18 show the CMC curves for IMP database for VIS-NIR matching of left periocular images, right periocular images and combined periocular images, respectively.

Figures 3.19, 3.20 and 3.21 show the CMC curves for PolyU database for VIS-NIR matching of left periocular images, right periocular images and combined periocular images, respectively.

Figures 3.22, 3.23 and 3.24 show the CMC curves for cross-eyed database for VIS-NIR matching of left periocular images, right periocular images and combined periocular images, respectively.

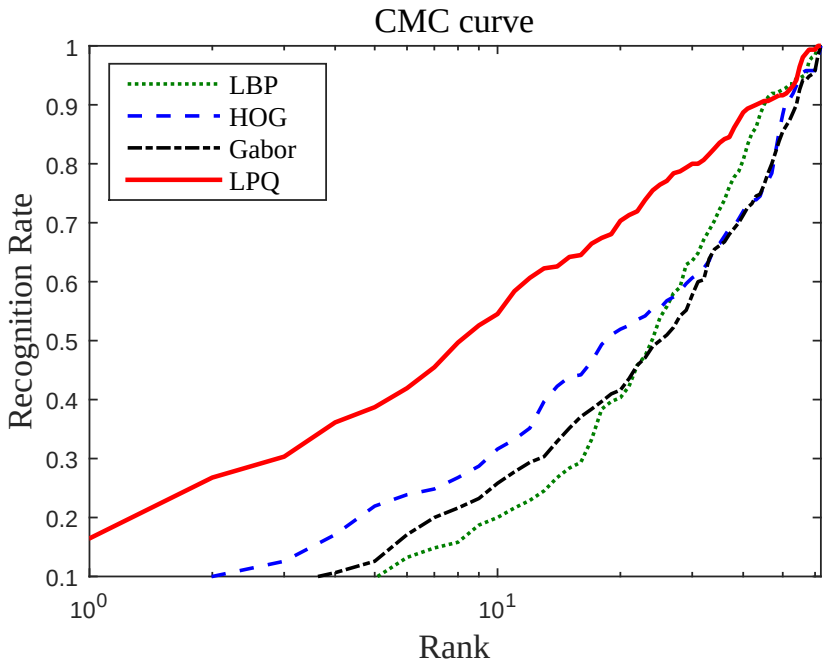

Figure 3.16: CMC curves for IMP database (Left periocular)

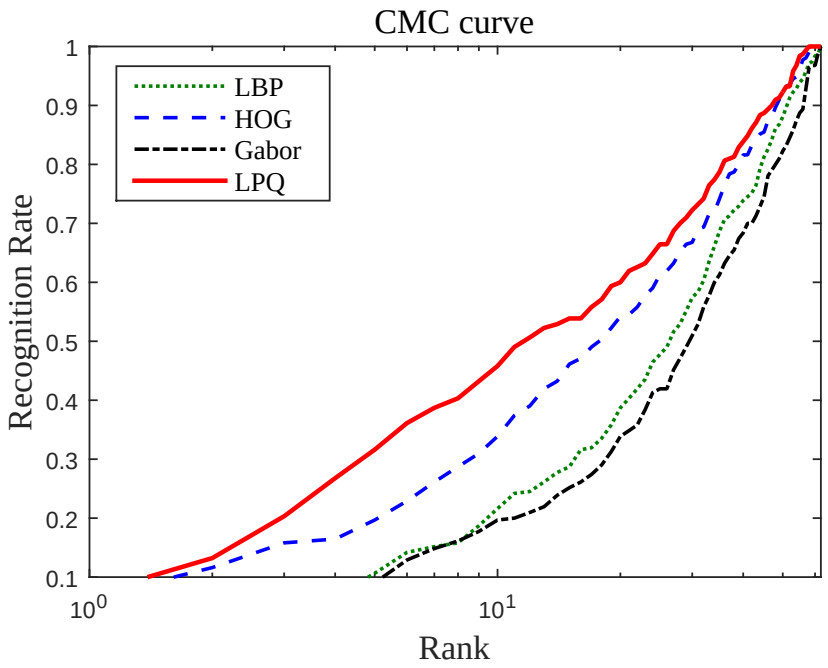

Figure 3.17: CMC curves for IMP database (Right periocular)

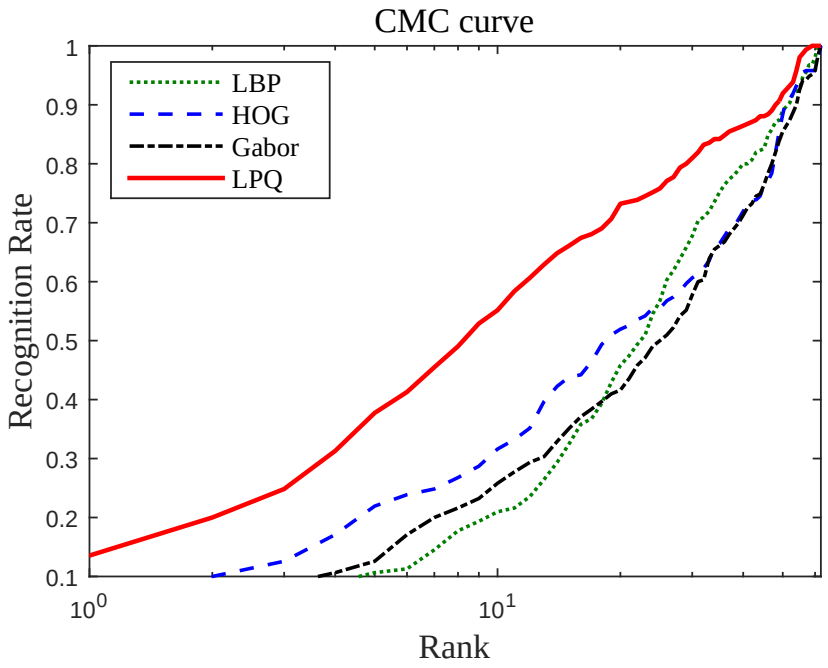

Figure 3.18: CMC curves for IMP database (Combined)

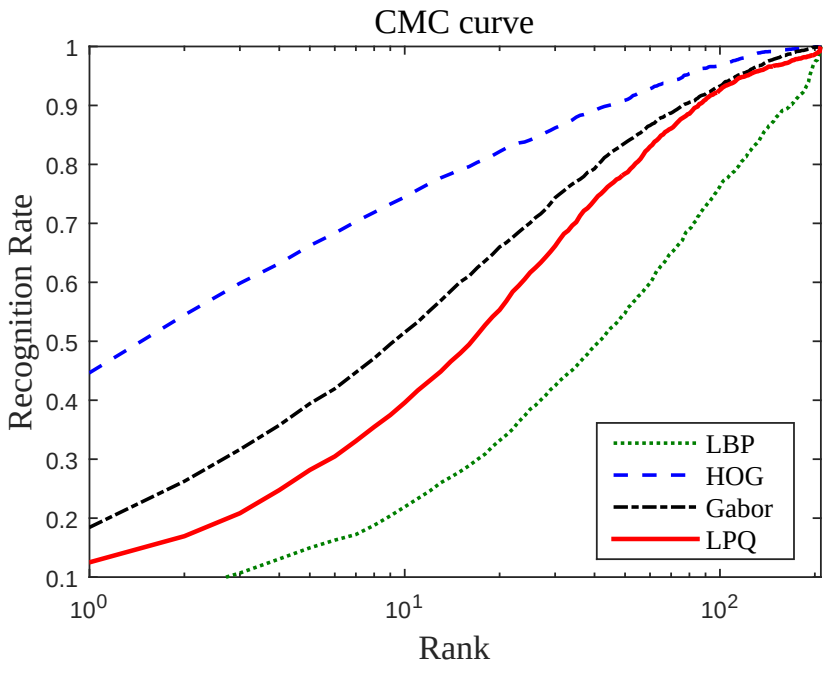

Figure 3.19: CMC curves for PolyU database (Left periocular)

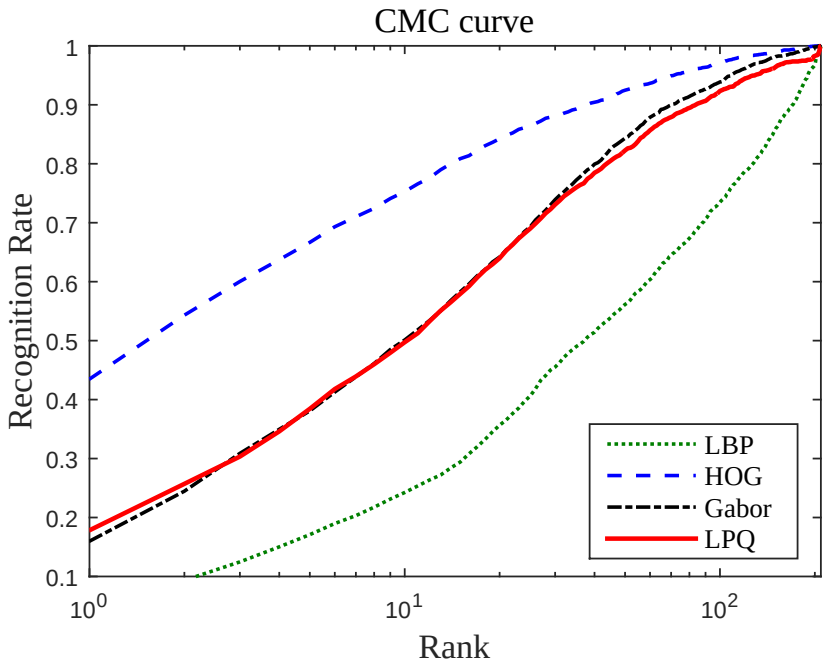

Figure 3.20: CMC curves for PolyU database (Right periocular)

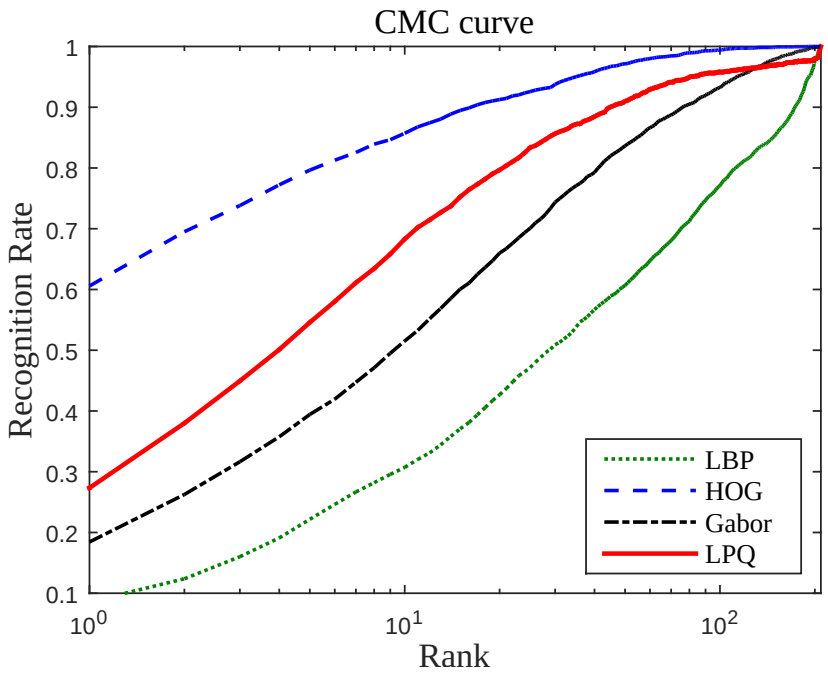

Figure 3.21: CMC curves for PolyU database (Combined)

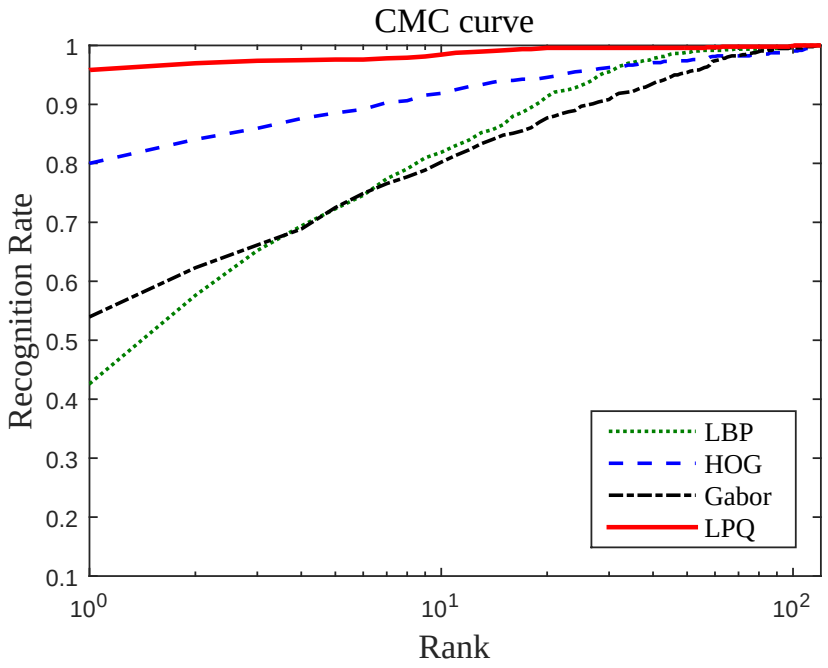

Figure 3.22: CMC curves for Cross-eyed database (Left periocular)

Figures 3.25, 3.26 and 3.27 show the CMC curves corresponding to VIS-NIR matching of left, right and combined periocular images belonging to image set 1.

Similarly, figures 3.28, 3.29 and 3.30 show the CMC curves corresponding to VIS-NIR matching of left, right and combined periocular images belonging to image set 2.

3.3 Discussion

Our experimental results suggest that reliable cross-spectral matching of periocular images can be performed with the proposed approach, which achieves best GARs (at 0.1 FAR) of 32.06%, 83.12% and 97.14% on IMP, PolyU and cross-eyed databases, respectively when both left and right periocular images are used for biometric verification. More importantly, the proposed method achieves state-of-the-art performance on the

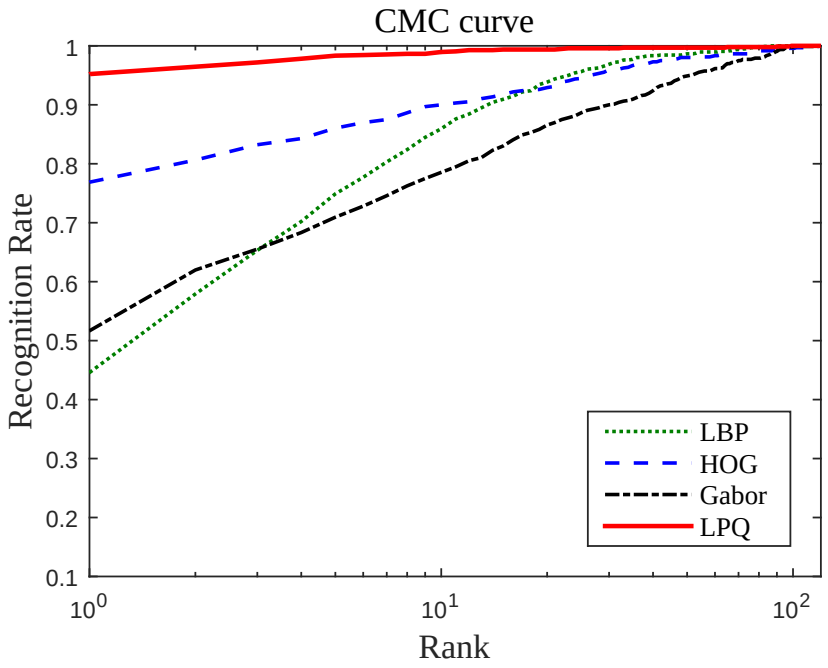

Figure 3.23: CMC curves for Cross-eyed database (Right periocular)

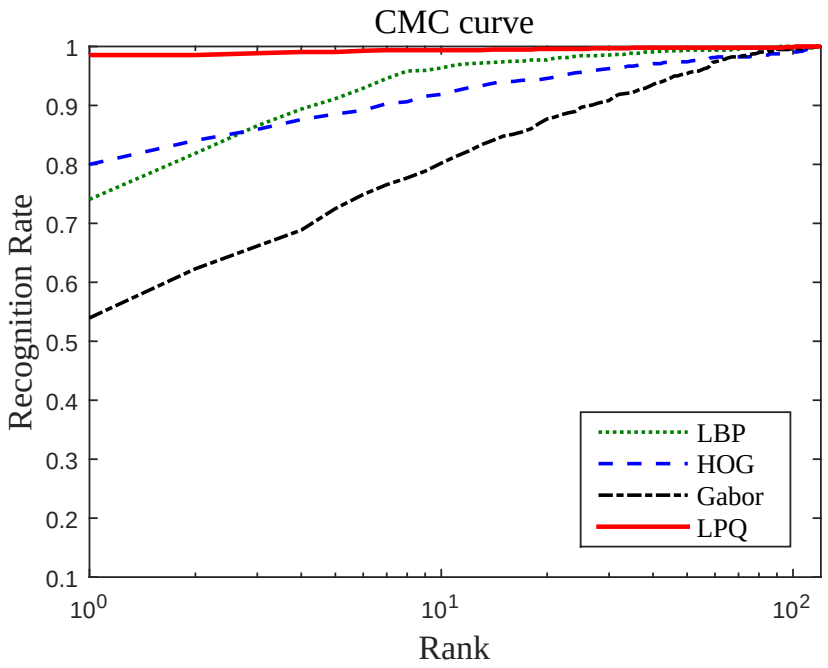

Figure 3.24: CMC curves for Cross-eyed database (Combined)

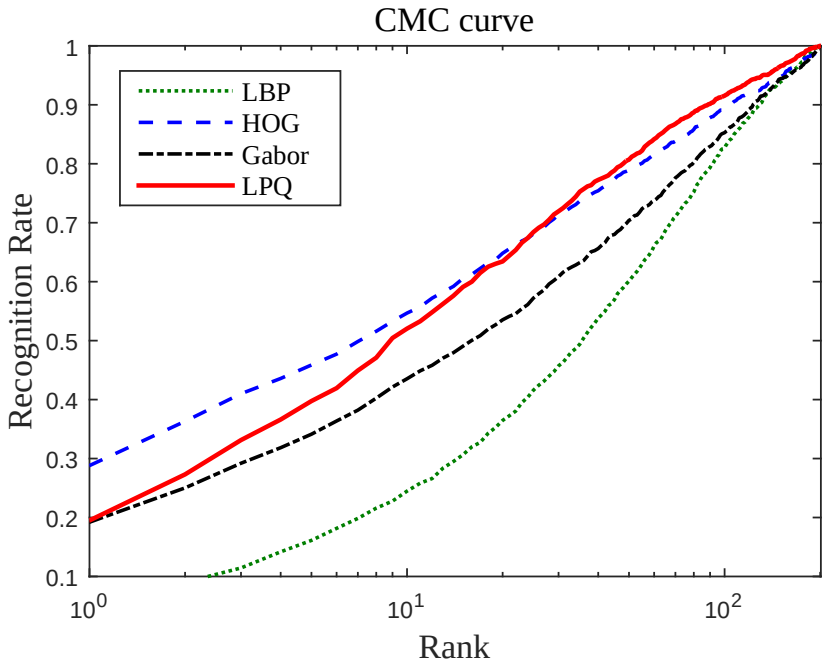

Figure 3.25: CMC curves for image set 1 (Left periocular)

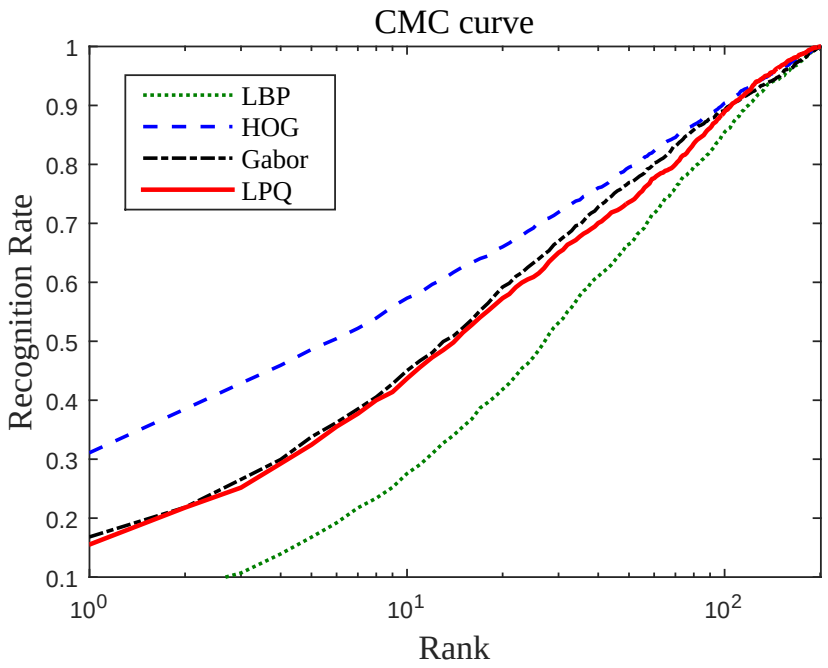

Figure 3.26: CMC curves for image set 1 (Right periocular)

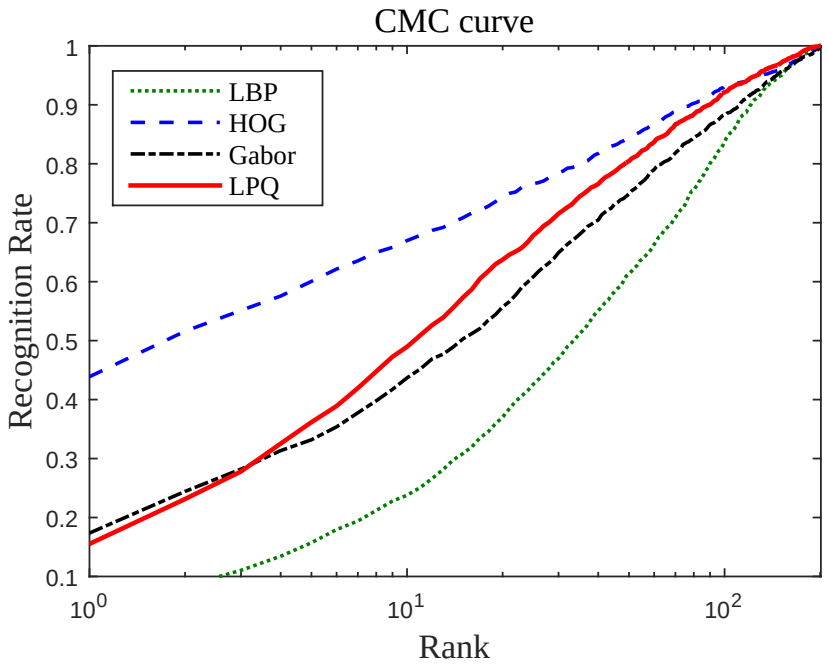

Figure 3.27: CMC curves for image set 1 (Combined)

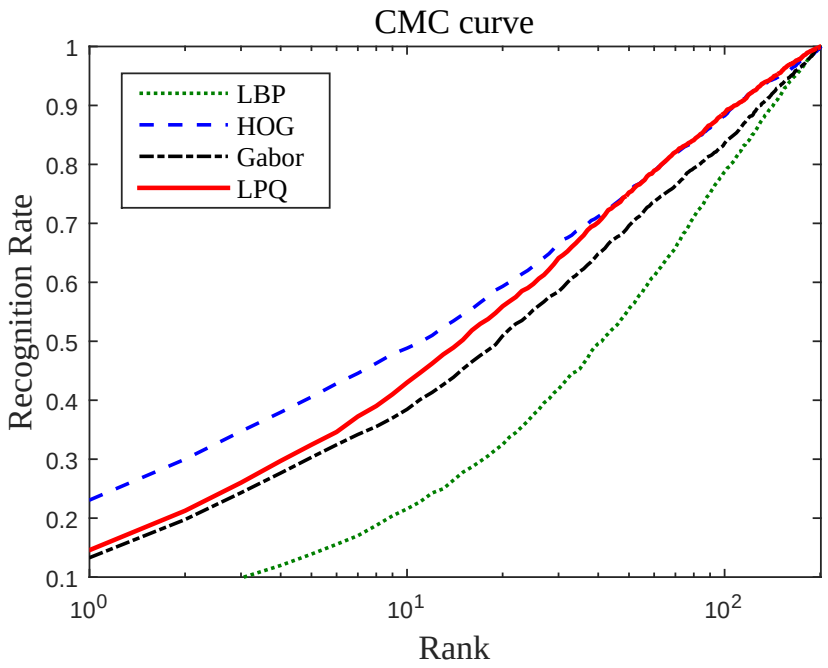

Figure 3.28: CMC curves for image set 2 (Left periocular)

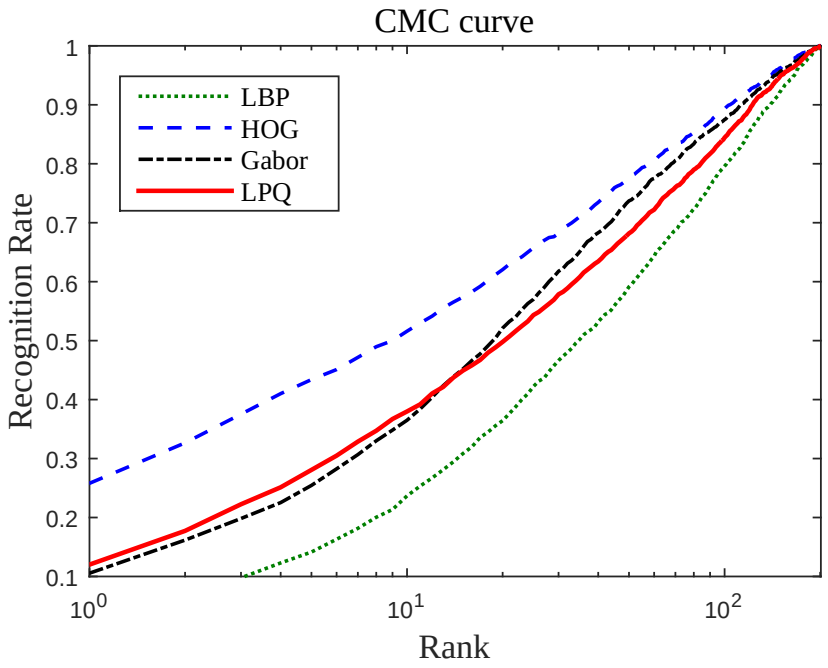

Figure 3.29: CMC curves for image set 2 (Right periocular)

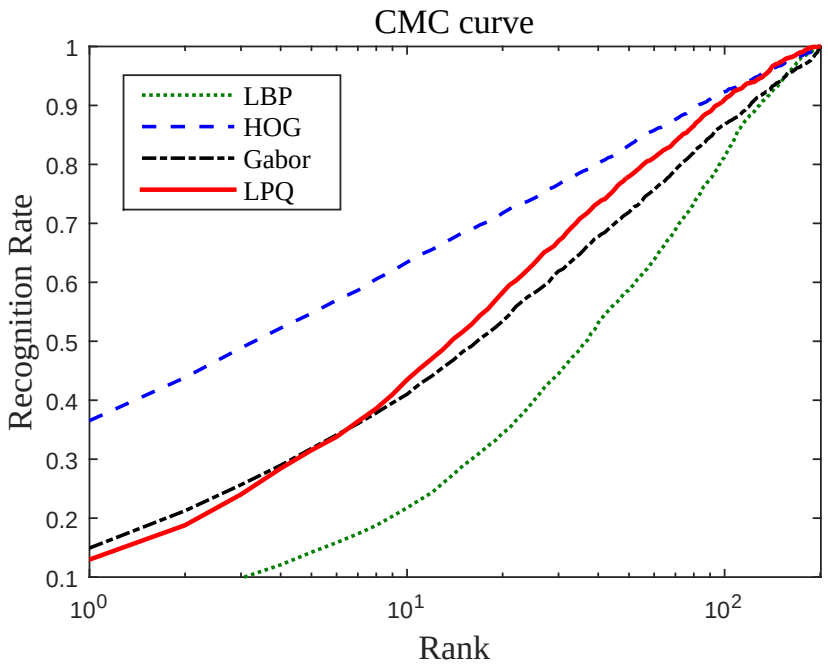

Figure 3.30: CMC curves for image set 2 (Combined)

publicly available PolyU dataset, with an improvement of nearly 10% points over the existing method. Similarly, our method achieves best rank-10 recognition rates of 55.16%, 85.71% and 99.38% for IMP, PolyU and cross-eyed databases, respectively when both left and right periocular images are used.

We have also compared the performance (in terms of verification accuracy) of the proposed approach with some of the existing illumination normalisation methods. The comparison results show satisfactory performance of the proposed approach while HOG is used as a feature vector.

The in-house database also performs satisfactorily for both verification and identification experiments (Tables 3.4 and 3.11). The proposed method achieves verification accuracies of 55.05% and 46.37% on image sets 1 and 2, respectively when HOG feature vectors are used. Similarly, the rank-10 recognition accuracies achieved on image sets 1 and 2 for HOG feature are 66.97% and 63.40%, respectively. Clearly, performance on image set 1 is more than that of image set 2 due to presence of higher quality images in it.

The performance of the proposed method on IMP database for both verification and identification scenarios is comparatively poor than that of other datasets. This is because the periocular images in the NIR domain are of poor quality and are not well aligned, due to which the performance degrades. On the other hand, the proposed method on cross-eyed database results in significantly higher verification and identification accuracies. The reason for this is the presence of perfectly aligned and high quality VIS and NIR periocular images.

Chapter 4

Conclusion and Future work

4.1 Conclusion

In this work, we have proposed a simple yet effective method for periocular recognition in cross-spectral scenarios. Our approach involves normalizing the images to reduce the effect of illumination variations. This is followed by the extraction of local texture descriptors and local shape descriptors and then comparison of the resultant feature vectors. In addition we have developed a new cross-spectral database consisting of periocular images of 201 subjects.

The performance of the proposed approach is evaluated on three publicly available periocular databases and also on the in-house database. Both verification and identification experiments are performed and results are presented on all four databases using four different feature descriptors and COS similarity measure. It is found that performance of the proposed approach on cross-eyed database achieves a GAR of 97.14% at 0.1 FAR and a rank-10 recognition rate of 99.38% for verification and identification scenarios respectively.

The in-house cross-spectral periocular database also gives satisfactory results for both verification and identification experiments. It achieves a verification accuracy of 55.05% at 0.1 FAR and a rank-10 recognition rate of 66.97%. It has also been observed

that the image set 2 has poor performance as compared to image set 1.

4.2 Future work

As part of our future work, we plan to ascertain the performance of the proposed approach on periocular images extracted from publicly available databases of heterogeneous facial images. We also plan to explore cross-spectral matching of periocular images acquired in other spectral bands.

In addition to the above, we look forward to developing efficient algorithms that yield improved performance for matching of cross-spectral periocular images of challenging databases such as IMP and the in-house database.

References

[1] N. P. Ramaiah and A. Kumar, "On matching cross-spectral periocular images for accurate biometric identification," in *8th IEEE International Conference on Biometrics: Theory, Applications, and Systems (BTAS)*, Sept 2016.

[2] I. Nigam, M. Vatsa, and R. Singh, "Ocular biometrics: A survey of modalities and fusion approaches," *Information Fusion*, vol. 26, pp. 1–35, 2015.

[3] S. Bharadwaj, H. S. Bhatt, M. Vatsa, and R. Singh, "Periocular biometrics: When iris recognition fails," in *Fourth IEEE International Conference on Biometrics: Theory Applications and Systems (BTAS)*, Sept 2010, pp. 1–6.

[4] G. Santos and H. Proena, "Periocular biometrics: An emerging technology for unconstrained scenarios," in *2013 IEEE Symposium on Computational Intelligence in Biometrics and Identity Management (CIBIM)*, April 2013, pp. 14–21.

[5] F. Juefei-Xu, D. K. Pal, and M. Savvides, "NIR-VIS heterogeneous face recognition via cross-spectral joint dictionary learning and reconstruction," in *IEEE Conference on Computer Vision and Pattern Recognition (CVPR) Workshops*, June 2015.

[6] T. Bourlai and B. Cukic, "Multi-spectral face recognition: Identification of people in difficult environments," in *IEEE International Conference on Intelligence and Security Informatics (ISI)*, June 2012, pp. 196–201.

[7] U. Park, A. Ross, and A. K. Jain, "Periocular biometrics in the visible spectrum: A feasibility study," in *3rd IEEE International Conference on Biometrics: Theory, Applications, and Systems (BTAS)*, Sept 2009, pp. 1–6.

[8] U. Park, R. R. Jillela, A. Ross, and A. K. Jain, "Periocular biometrics in the visible spectrum," *IEEE Transactions on Information Forensics and Security*, vol. 6, no. 1, pp. 96–106, March 2011.

[9] L. Nie, A. Kumar, and S. Zhan, "Periocular recognition using unsupervised convolutional RBM feature learning," in *Pattern Recognition (ICPR), 22nd International Conference on.* IEEE, 2014, pp. 399–404.

[10] C. N. Padole and H. Proenca, "Periocular recognition: Analysis of performance degradation factors," in *2012 5th IAPR International Conference on Biometrics (ICB)*, March 2012, pp. 439–445.

[11] F. Alonso-Fernandez and J. Bigun, "Near-infrared and visible-light periocular recognition with gabor features using frequency-adaptive automatic eye detection," *IET Biometrics*, vol. 4, no. 2, pp. 74–89, 2015.

[12] M. Uzair, A. Mahmood, A. Mian, and C. McDonald, "Periocular region-based person identification in the visible, infrared and hyperspectral imagery," *Neurocomputing*, vol. 149, pp. 854–867, 2015.

[13] P. E. Miller, A. W. Rawls, S. J. Pundlik, and D. L. Woodard, "Personal identification using periocular skin texture," in *Proceedings of the ACM Symposium on Applied Computing.* ACM, 2010, pp. 1496–1500.

[14] D. L. Woodard, S. J. Pundlik, J. R. Lyle, and P. E. Miller, "Periocular region appearance cues for biometric identification," in *Computer Vision and Pattern Recognition Workshops (CVPRW), IEEE Computer Society Conference on.* IEEE, 2010, pp. 162–169.

[15] G. Mahalingam and K. Ricanek, "LBP-based periocular recognition on challenging face datasets," *EURASIP Journal on Image and Video processing*, vol. 2013, no. 1, p. 36, 2013.

[16] J. Xu, M. Cha, J. L. Heyman, S. Venugopalan, R. Abiantun, and M. Savvides, "Robust local binary pattern feature sets for periocular biometric identification," in *Biometrics: Theory Applications and Systems (BTAS), Fourth IEEE International Conference on*. IEEE, 2010, pp. 1–8.

[17] Ş. Karahan, A. Karaöz, Ö. F. Özdemir, A. G. Gü, and U. Uludag, "On identification from periocular region utilizing SIFT and SURF," in *Signal Processing Conference (EUSIPCO), Proceedings of the 22nd European*. IEEE, 2014, pp. 1392–1396.

[18] B.-S. Oh, K. Oh, and K.-A. Toh, "On projection-based methods for periocular identity verification," in *Industrial Electronics and Applications (ICIEA), 7th IEEE Conference on*. IEEE, 2012, pp. 871–876.

[19] F. Alonso-Fernandez and J. Bigun, "Periocular recognition using retinotopic sampling and Gabor decomposition," in *Computer Vision–ECCV, Workshops and Demonstrations*. Springer, 2012, pp. 309–318.

[20] A. Mikaelyan, F. Alonso-Fernandez, and J. Bigun, "Periocular recognition by detection of local symmetry patterns," in *Signal-Image Technology and Internet-Based Systems (SITIS), Tenth International Conference on*. IEEE, 2014, pp. 584–591.

[21] A. Gangwar and A. Joshi, "Robust periocular biometrics based on local phase quantisation and Gabor transform," in *Image and Signal Processing (CISP), 7th International Congress on*. IEEE, 2014, pp. 714–720.

[22] A. Joshi, A. Gangwar, R. Sharma, A. Singh, and Z. Saquib, "Periocular recognition based on Gabor and Parzen PNN," in *Image Processing (ICIP), IEEE International Conference on*. IEEE, 2014, pp. 4977–4981.

[23] F. Alonso-Fernandez and J. Bigun, "A survey on periocular biometrics research," *Pattern Recognition Letters*, vol. 82, pp. 92–105, 2016.

[24] M. Uzair, A. Mahmood, A. Mian, and C. McDonald, "Periocular biometric recognition using image sets," in *IEEE Workshop on Applications of Computer Vision (WACV)*, Jan 2013, pp. 246–251.

[25] K. P. Hollingsworth, S. S. Darnell, P. E. Miller, D. L. Woodard, K. W. Bowyer, and P. J. Flynn, "Human and machine performance on periocular biometrics under near-infrared light and visible light," *IEEE Transactions on Information Forensics and Security*, vol. 7, no. 2, pp. 588–601, April 2012.

[26] F. Alonso-Fernandez, A. Mikaelyan, and J. Bigun, "Comparison and fusion of multiple iris and periocular matchers using near-infrared and visible images," in *International Workshop on Biometrics and Forensics (IWBF)*, March 2015, pp. 1–6.

[27] G. Santos, E. Grancho, M. V. Bernardo, and P. T. Fiadeiro, "Fusing iris and periocular information for cross-sensor recognition," *Pattern Recognition Letters*, vol. 57, pp. 52–59, 2015.

[28] R. Raghavendra, K. B. Raja, B. Yang, and C. Busch, "Combining iris and periocular recognition using light field camera," in *Pattern Recognition (ACPR), 2nd IAPR Asian Conference on*. IEEE, 2013, pp. 155–159.

[29] K. B. Raja, R. Raghavendra, and C. Busch, "Binarized statistical features for improved iris and periocular recognition in visible spectrum," in *Biometrics and Forensics (IWBF), International Workshop on*. IEEE, 2014, pp. 1–6.

[30] D. L. Woodard, S. Pundlik, P. Miller, R. Jillela, and A. Ross, "On the fusion of periocular and iris biometrics in non-ideal imagery," in *Pattern Recognition (ICPR), 20th International Conference on.* IEEE, 2010, pp. 201–204.

[31] C.-W. Tan and A. Kumar, "Human identification from at-a-distance images by simultaneously exploiting iris and periocular features," in *Pattern Recognition (ICPR), 21st International Conference on.* IEEE, 2012, pp. 553–556.

[32] J. R. Lyle, P. E. Miller, S. J. Pundlik, and D. L. Woodard, "Soft biometric classification using local appearance periocular region features," *Pattern Recognition*, vol. 45, no. 11, pp. 3877–3885, 2012.

[33] ——, "Soft biometric classification using periocular region features," in *Biometrics: Theory Applications and Systems (BTAS), Fourth IEEE International Conference on.* IEEE, 2010, pp. 1–7.

[34] G. Mahalingam, K. Ricanek, and A. M. Albert, "Investigating the periocular-based face recognition across gender transformation," *IEEE Transactions on Information Forensics and Security*, vol. 9, no. 12, pp. 2180–2192, 2014.

[35] H. Maeng, H.-C. Choi, U. Park, S.-W. Lee, and A. K. Jain, "NFRAD: Near-infrared face recognition at a distance," in *International Joint Conference on Biometrics (IJCB)*, Oct 2011, pp. 1–7.

[36] J.-Y. Zhu, W.-S. Zheng, J.-H. Lai, and S. Z. Li, "Matching NIR face to VIS face using transduction," *IEEE Transactions on Information Forensics and Security*, vol. 9, no. 3, pp. 501–514, 2014.

[37] A. Ross, R. Pasula, and L. Hornak, "Exploring multispectral iris recognition beyond 900nm," in *IEEE 3rd International Conference on Biometrics: Theory, Applications, and Systems (BTAS).*, Sept 2009, pp. 1–8.

[38] J. Zuo, F. Nicolo, and N. A. Schmid, "Cross spectral iris matching based on predictive image mapping," in *IEEE 4th International Conference on Biometrics: Theory, Applications, and Systems (BTAS)*, Sept 2010, pp. 1–5.

[39] N. Ramaiah and A. Kumar, "Towards more accurate iris recognition using cross-spectral matching," *IEEE Transactions on Image Processing*, vol. PP, no. 99, pp. 1–1, 2016.

[40] A. Sharma, S. Verma, M. Vatsa, and R. Singh, "On cross spectral periocular recognition," in *IEEE International Conference on Image Processing (ICIP)*, Oct 2014, pp. 5007–5011.

[41] Z. X. Cao and N. A. Schmid, "Matching heterogeneous periocular regions: Short and long standoff distances," in *IEEE International Conference on Image Processing (ICIP)*, Oct 2014, pp. 4967–4971.

[42] Z. Cao and N. A. Schmid, "Fusion of operators for heterogeneous periocular recognition at varying ranges," *Pattern Recognition Letters*, vol. 82, pp. 170–180, 2016.

[43] ——, "Recognition performance of cross-spectral periocular biometrics and partial face at short and long standoff distance," *Open Trans. Inf. Process*, vol. 1, no. 2, pp. 20–32, 2014.

[44] T. Ojala, M. Pietikainen, and T. Maenpaa, "Multiresolution gray-scale and rotation invariant texture classification with local binary patterns," *IEEE Transactions on Pattern Analysis and Machine Intelligence*, vol. 24, no. 7, pp. 971–987, Jul 2002.

[45] N. Dalal and B. Triggs, "Histograms of oriented gradients for human detection," in *IEEE Computer Society Conference on Computer Vision and Pattern Recognition (CVPR)*. IEEE, 2005, pp. 886–893.

[46] V. Ojansivu and J. Heikkilä, "Blur insensitive texture classification using local phase quantization," in *International conference on image and signal processing*. Springer, 2008, pp. 236–243.

[47] A. K. Jain, N. K. Ratha, and S. Lakshmanan, "Object detection using Gabor filters," *Pattern recognition*, vol. 30, no. 2, pp. 295–309, 1997.

[48] P. Viola and M. J. Jones, "Robust real-time face detection," *International journal of computer vision*, vol. 57, no. 2, pp. 137–154, 2004.

[49] A. Sequeira, L. Chen, P. Wild, J. Ferryman, F. Alonso-Fernandez, K. B. Raja, R. Raghavendra, C. Busch, and J. Bigun, "Cross-eyed - cross-spectral iris/periocular recognition database and competition," in *International Conference of the Biometrics Special Interest Group (BIOSIG)*, Sept 2016, pp. 1–5.

[50] K. Kohlmann, "Corner detection in natural images based on the 2-D hilbert transform," *Signal Processing*, vol. 48, no. 3, pp. 225–234, 1996.

[51] A. M. Reza, "Realization of the contrast limited adaptive histogram equalization (CLAHE) for real-time image enhancement," *Journal of VLSI signal processing systems for signal, image and video technology*, vol. 38, no. 1, pp. 35–44, 2004.

[52] D. J. Jobson, Z. Rahman, and G. A. Woodell, "Properties and performance of a center/surround retinex," *IEEE Transactions on Image Processing*, vol. 6, no. 3, pp. 451–462, Mar 1997.

List of Publications

- Sushree Behera, Mahesh Gour, Vivek Kanhangad and Niladri Puhan, "Periocular recognition in cross-spectral scenario.", *International Joint Conference on Biometrics (IJCB)*,Oct 2017, Denver, USA. (Accepted)

- Ana F. Sequeira, Lulu Chen, James Ferryman, Peter Wild, Fernando Alonso-Fernandez, Josef Bigun, Tiago de Freitas Pereira, Sebastien Marcel, **Sushree Sangeeta Behera**, **Mahesh Gour**, **Vivek Kanhangad**, Kiran B. Raja, R. Raghavendra, Christoph Busch, "Cross-Eyed - Cross-Spectral Iris/Periocular Recognition Competition", *International Joint Conference on Biometrics (IJCB)*, Oct 2017. (Secured 7th position)